

1 *Introducing relative pollen productivity estimates for Iberian taxa:
2 methodological insights and implications for landscape modelling in the
3 Western Mediterranean*

4 Kilian Jungkeit-Milla^{1,2*+}, Vojtěch Abraham^{3,4*}, Miguel Sevilla-Callejo¹, Xavier Font⁵,
5 Héctor Romanos^{1(†)}, Eduardo García-Prieto¹, Josu Aranbarri⁶, María Leunda⁷, Michelle
6 Farrell⁸, Fátima Franco-Múgica⁹, Michela Mariani¹⁰, Florence Mazier¹¹, Helios Sainz-
7 Ollero⁹, Penélope González-Sampériz¹⁺ and Graciela Gil-Romera¹⁺

8 ¹Pyrenean Institute of Ecology-CSIC, Zaragoza, Spain. ²Department of Geography and Regional Planning, University of Zaragoza.

9 ³Department of Botany, Charles University in Prague, Prague, Czech Republic. ⁴Czech Academy of Sciences, Institute of Botany,
10 Department of Paleoecology, Brno, Czech Republic. ⁵Faculty of Biology, University of Barcelona, Barcelona, Spain. ⁶Department of
11 Geography, Prehistory and Archaeology, University of the Basque Country, Vitoria-Gasteiz, Spain. ⁷ Institute of Plant Sciences and
12 Oeschger Center for Climate Change Research, University of Bern, Bern, Switzerland. ⁸ Centre for Agroecology, Water and
13 Resilience, Coventry University, Coventry, United Kingdom. ⁹ Faculty of Sciences. Autonomous University of Madrid, Madrid,
14 Spain. ¹⁰ School of Geography, University of Nottingham, Nottingham, United Kingdom. ¹¹ Department of Environmental Geography,
15 Université Toulouse II - Jean Jaurès, UTM · UMR Laboratoire GÉODE, France.

16 * These two authors share the first authorship

17 [†] Deceased in 2023.

18 +Correspondence: Kilian Jungkeit-Milla (kilian@ipe.csic.es), Penélope González-Sampériz (pgonzal@ipe.csic.es) and Graciela Gil-
19 Romera (graciela.gil@ipe.csic.es)

20 Note: nomenclature and authority of the taxa in this paper were selected according to Flora Iberica (Castroviejo, 2012).

21 **Abstract**

22 Understanding the impact of ongoing global change on plant communities requires long-term
23 quantitative reconstructions of past vegetation dynamics. Fossil pollen records offer one of the
24 most powerful tools to reconstruct past landscapes, yet for their accurate interpretation it is
25 important to take into account the differential pollen productivity of plant taxa. For southern
26 Europe, and particularly for the Iberian Peninsula, estimates of pollen productivity remain scarce,
27 limiting our ability to refine palaeoecological reconstructions.

28 Here we present the first relative pollen productivity estimates (RPPs) for 21 common taxa in
29 continental Spain. For that purpose, we used 1,113 modern pollen samples from own surveys and
30 the Eurasian Modern Pollen Database (EMPD2), and vegetation data from the Spanish Forestry
31 Map (MFE) and the Iberian and Macaronesian Vegetation Information System (SIVIM). RPPs
32 were derived by applying an optimisation algorithm with the REVEALS model (REgional
33 VEgetation Estimates from Large Sites). To test the reliability of our RPPs, we validated 8
34 arboreal taxa in 26 present-day coretops across Spain. We also compared the obtained RPPs with
35 different studies across Europe, using a bias-free comparison framework.

36 Our findings indicate that the dominant arboreal taxa (*Pinus*, evergreen and deciduous *Quercus*)
37 are high pollen producers, whereas temperate forest, shrub and herbaceous taxa generally yielded
38 medium to low estimates of pollen productivity. Validation of the most frequent taxa from
39 present-day coretops showed that REVEALS-based estimates perform better than raw pollen
40 counts when compared with present-day vegetation cover. Comparison between different studies
41 in Europe also showed that most of the Spanish RPPs are similar to those obtained in Europe,
42 although notable differences emerged for some taxa.

43 This study calculates, validates and compares the first RPPs in the Western Mediterranean,
44 highlighting the value of quantitative palaeoecological data for Holocene landscape
45 reconstructions. The findings of this paper would support that the Iberian Peninsula could have

46 been home to a heterogeneous mosaic of open areas, conifers and broadleaf trees, offering new
47 frameworks to improve both palaeoecological reconstructions and contemporary forest
48 management strategies.

49 **Keywords:** RPPs, PPEs, REVEALS, Mediterranean basin, land cover, palaeoecology.

50 **1. Introduction**

51 Science for mitigation and adaptation to global change needs to quantify how much landscapes
52 changed under the pressure of climate variability and human agency. Acquiring a numerically
53 detailed understanding of changes in land use and vegetation cover through time is crucial to
54 establish reliable environmental models of the impacts of past climate change on plant
55 communities.

56 Likewise, land cover reconstructions are crucial elements for answering various ecological
57 questions and changes in land use (Fyfe et al., 2015; Pearce et al., 2023; Roberts et al., 2018;
58 Trondman et al., 2014; Woodbridge et al., 2019). A central challenge in palaeoecology is to
59 determine not only how vegetation cover varied in space and time, but also how these changes
60 interacted with the physical environment and disturbance regimes. This involves asking key
61 palaeoecological questions shaped by some of the long-standing debates over the historical
62 structure and dynamics of European landscapes. Some influential and controversial hypotheses
63 (e.g., Svenning, 2002; Vera, 2000) dispute the traditional view of densely forested wilderness.
64 Instead, they propose that large herbivores and disturbance regimes maintained extensive areas
65 of semi-open habitats across much of postglacial Europe. This debate continues today, supported
66 by robust palaeoecological data used to evaluate these hypotheses (Pearce et al., 2023). Recent
67 studies increasingly suggest that postglacial Europe had a mixed composition of both closed
68 forests and open areas (Carrión et al., 2010a; Nikulina et al., 2024; Pearce et al., 2025a),
69 highlighting that the drivers of vegetation openness extend beyond climatic and human influences
70 and emphasising the significant roles of large herbivores (Pearce et al., 2025b)

71 Accurate reconstruction of forest structure and baseline conditions for ecological restoration
72 largely depends on pollen-based land cover reconstructions, which are not only vital for
73 unravelling the long-term interplay between ecological and human processes, but also for
74 producing reliable regional and global climate models and biogeochemical cycles (Abrantes et
75 al., 2012; Cheddadi et al., 1998; Li et al., 2011; Liu et al., 2023). Integrating quantitative pollen
76 data with diachronic cartography and multi-proxy evidence is also crucial to reconstruct the
77 effects of past disturbances (Githumbi et al., 2022; Pirzamanbein et al., 2014, 2020; Zanon et al.,
78 2018) – including fire, human deforestation and herbivory – allowing us to quantify biomass
79 affected over time and the spatial extent of disturbance regimes and disentangle overlapping
80 effects of natural and anthropogenic drivers (Ellis, 2021; Morrison et al., 2021; Nikulina et al.,
81 2024; Pearce et al., 2025b).

82 In this regard, pollen records are the most widely used proxies for past vegetation reconstruction
83 (Andersen, 1970; Broström et al., 2008; Davis, 1963; Huntley, 1990; Sugita, 1994; Von Post,
84 1918). Indeed, one of the main goals of pollen analysis is to reconstruct past plant abundances.
85 However, it has long been known that there is a lack of linearity between pollen presence and
86 abundance of the producing plant taxa (Andersen, 1970; Davis, 1963; Prentice and Parsons, 1983;
87 Sugita, 1994), resulting in some taxa being overrepresented in fossil pollen records due to their
88 high productivity and effective dispersal, while others may be underrepresented owing to low
89 productivity and limited dispersal capacity (Davis, 1963). This discrepancy can lead to biased
90 reconstructions of past vegetation and land cover (Prentice and Webb, 2009; Sugita, 1994). Thus,
91 rigorous estimation of the composition of past vegetation relies on our ability to better

92 comprehend and quantify the relationships between fossil pollen assemblages and the
93 composition of the vegetation that produces them.

94 A first step in the quantitative reconstruction of Quaternary vegetation using fossil pollen records
95 requires calculating the pollen productivity estimates (PPEs), or relative pollen productivity
96 estimates (RPPs), for the taxa whose land cover we aim to reconstruct. Pollen productivity is often
97 defined as the number of pollen grains produced per unit relative abundance of a given taxon, and
98 is usually expressed as a dimensionless ratio relative to a reference taxon, since absolute pollen
99 production measurement is difficult to determine (Andersen, 1970). RPPs are one of the critical
100 parameters required to produce a reliable model of past vegetation abundance, as they enable
101 correction of under or over estimations of taxa abundance.

102 Relative pollen productivity estimates (hereafter referred to as RPPs) have been calculated for
103 many regions of northern and central Europe in the last decades (Abraham and Kozáková, 2012;
104 Baker et al., 2016; Broström et al., 2004; Bunting et al., 2005; Grin Dean et al., 2019; Hjelle, 1998;
105 Kuneš et al., 2019; Mazier et al., 2008; Nielsen, 2004; Niemeyer et al., 2015; Poska et al., 2011;
106 Soepboer et al., 2007; Theuerkauf et al., 2013). RPPs have also been calculated in the eastern
107 Mediterranean (Ergin et al., 2024), as well as in North America (Calcote, 1995; Chaput and
108 Gajewski, 2018; Commerford et al., 2013), Africa (Duffin and Bunting, 2008; Tabares et al.,
109 2021), Asia (Han et al., 2017; He et al., 2016; Jiang et al., 2020) and Oceania (Mariani et al.,
110 2016, 2022). Despite the abundance of RPP studies for different taxa in mid or high European
111 latitudes, other regions of the world remain understudied. One example is the five Mediterranean-
112 climate regions (MCRs) of the world. Despite occupying less than 5% of the Earth's surface, they
113 host about 48,250 known vascular plant species (Cowling et al., 1996) and yet, there are very few
114 RPPs existing in these areas (Ergin et al., 2024; Githumbi et al., 2022). The MCRs also represent
115 a critical biome for understanding long-term human-landscape relationships as the Mediterranean
116 Basin in particular represents a very long history of human occupation and therefore ecosystem
117 change, resilience or persistence, besides a particularly vulnerable scenario regarding current
118 global change and future warming (IPCC, 2023). The lack of RPPs for MCRs precludes any
119 quantitative land cover reconstruction from fossil records in these areas, although efforts have
120 been recently made to obtain new RPPs for some Mediterranean areas (Ergin et al., 2024;
121 Githumbi et al., 2022; Serge et al., 2023). The fact that all previous numerical approaches have
122 been conducted in mixed temperate forests or in subtropical areas implies that the complexity of
123 Mediterranean plant communities has rarely been considered in these attempts.

124 Some of the available RPPs for northern European taxa could potentially be of use in the
125 Mediterranean basin, but it is well-known that pollen productivity might be driven by a number
126 of geographical factors, plant taxonomy and climate constraints (Baker et al., 2016; Broström et
127 al., 2004, 2008). Often, RPPs for the same taxa may differ due to methodological issues at the
128 data resolution and landscape characterisation level, and from a number of methodological
129 assumptions (Liu et al., 2022). These inconsistencies challenge the transferability of RPPs beyond
130 their original context and, consequently, their application is often restricted to localised settings
131 (Liu et al., 2022). Essentially, having a robust estimate of pollen productivity for taxa of a
132 particular region implies considering all these factors and thus obtaining new RPPs.

133 In the present work, our objectives are: 1) to produce RPPs for 21 woody and herbaceous taxa
134 across the Spanish Territory of Iberia (STI, from now on), 2) to validate the obtained results using
135 present-day pollen samples from coretops within the region and 3) to compare our results with
136 those from other European RPP studies. STI holds one of the greatest ecosystem, habitat and plant
137 species diversities of Europe (Maestre et al., 2021; Médail and Quézel, 1999; Mutke et al., 2010)

138 and comprises two biogeographical domains: the Mediterranean region, which accounts for about
139 70% of the STI, and the Eurosiberian region, located in the northernmost areas of the STI (~30%).
140 Our work is the first comprehensive study conducted in Iberia to obtain relative pollen
141 productivity estimates, and it represents the first step towards the quantitative reconstruction of
142 past landscapes framework in the Western Mediterranean, and particularly in STI.

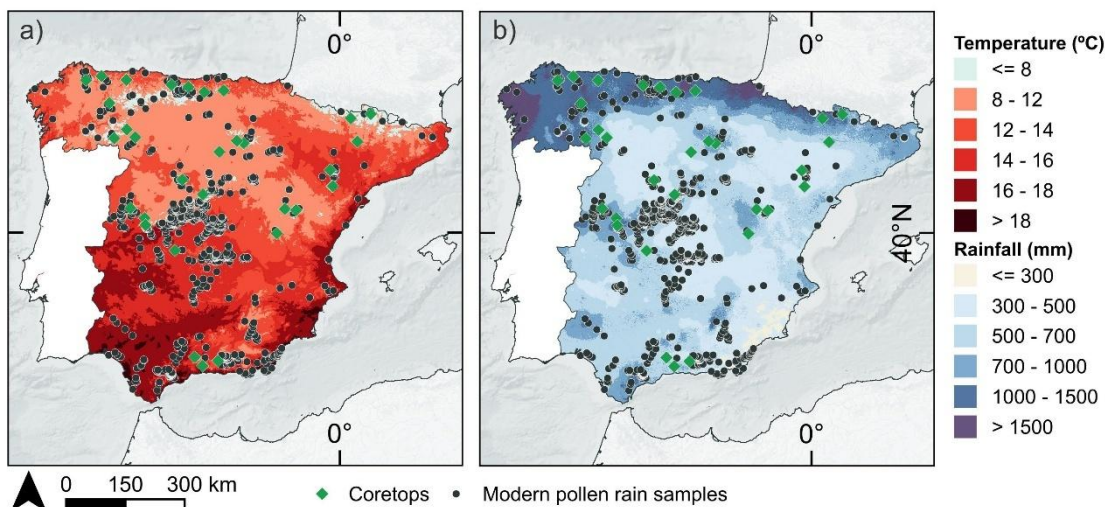
143 **2. Material and methods**

144 **2.1 Study area**

145 The study area covers the whole of continental Spain (504.782 km^2) including the two
146 biogeographical regions, Eurosiberian and Mediterranean.

147 *a) Mediterranean bioclimatic region*

148 The Mediterranean region extends throughout most of the STI, covering all of the central and
149 eastern region except for the mountain and alpine areas. STI exhibits remarkable climatic
150 diversity, largely driven by its complex topography and geographic position. Mean annual
151 temperatures (MAT) range from approximately 8°C in the interior plateaus and mountainous
152 regions to around 18°C along the Mediterranean coast (Fig.1). In alpine zones of the
153 Mediterranean, MAT often falls below 8°C . Precipitation patterns are equally heterogeneous:
154 while the national mean annual precipitation (MAP) is around 500 mm, values vary widely—
155 from 1000–1500 mm in mountainous areas to as low as 200–600 mm in coastal and plateau
156 regions (Chazarra et al., 2018) (Fig. 1). This climatic variability underpins the country's
157 exceptional ecological and floristic diversity, resulting in a variety of habitats and landscapes.



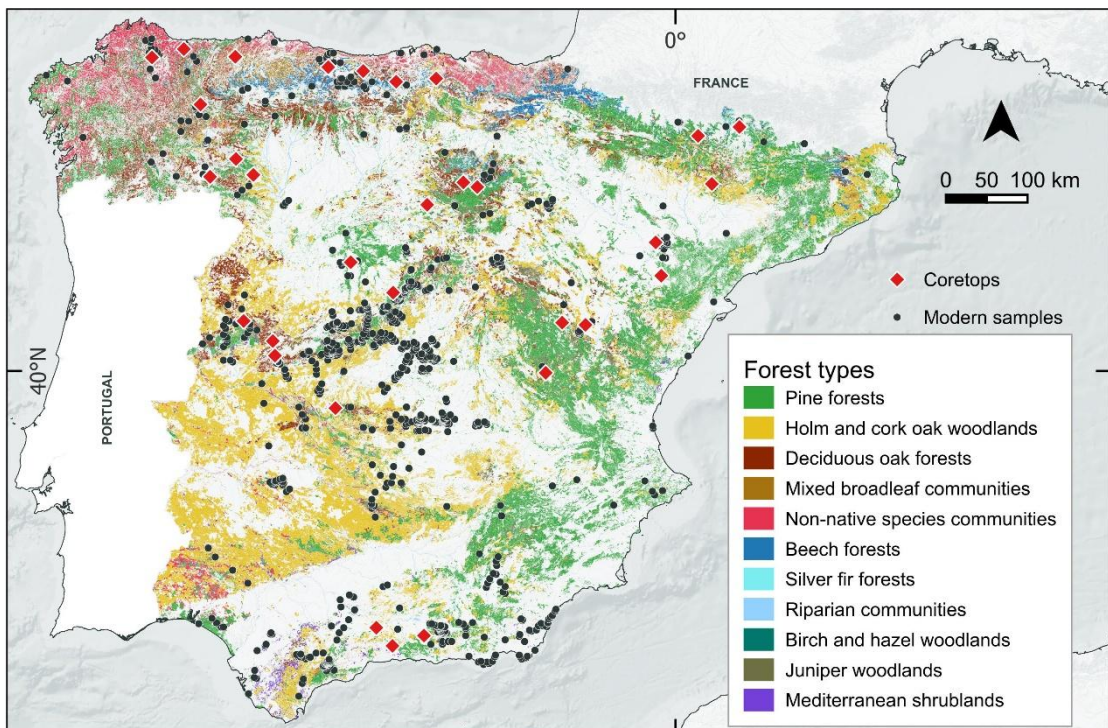
159 Figure 1. a) Mean annual temperature (MAT, $^\circ\text{C}$) and b) mean annual precipitation (MAP, mm) in continental Spain
160 (Ninyerola et al., 2005). Black dots represent the locations of the surface samples used in this study; green squares
161 represent the coretops used for validation.

162 Mediterranean forest ecosystems cover two thirds of the total wooded region in the STI (Costa et
163 al., 1998). These woody communities are physiognomically diverse and vary from scrub to dense
164 mature forests, and from thorny, macchia-like temperate steppes to cold semi-deserts (Costa et
165 al., 1998; Gavilán et al., 2018). Mediterranean forests, structured along a marked altitudinal
166 gradient, are predominantly monospecific, although they are occasionally mixed with other
167 woody species. These are mainly evergreen sclerophyllous taxa, though sometimes deciduous
168 taxa are also present (Fig. 2).

169 In coastal and lowland areas (0-400 m asl) macchia and garrigue-type shrublands, grasslands and
170 forests of different species of *Pinus* (*P. halepensis* Mill., *P. pinaster* Aiton, *P. pinea* L.) are
171 dominant. Some other pines can also be found in the Mediterranean foothills and mountain belts
172 (400-1200 m asl): *P. sylvestris* L. (Scots pine), *P. nigra* subsp. *salzmanii* (Dunal) Franco, *P. nigra*
173 subsp. *nigra* J.F. Arnold. (black pine) and those from lowland areas, along with the main oak taxa
174 of Mediterranean sclerophyllous forests, *Quercus ilex* L. and *Q. suber* L. (holm and cork oak
175 woodlands, Fig. 2). These forests appear often combined with *Juniperus* spp. communities (*J.
176 thurifera* L., *J. phoenicea* L., *J. communis* L., *J. oxycedrus* L., or *J. sabina* L.), which are quite
177 characteristic of the plateau-continental STI, including open areas that rarely form continuous
178 canopy forests. Oak, pine and juniper communities are all adapted to periods of aridity that may
179 vary from two to nine months of the year. Some woodlands in the Mediterranean mountains also
180 support deciduous taxa such as birch (*Betula pendula* Roth., *B. alba* L.) and ash (*Fraxinus
181 excelsior* Vahl., *F. angustifolia* L.), as well as some semi-deciduous oak species as *Q. faginea*
182 Lam., and *Q. pyrenaica* Willd. Relics of *Abies pinsapo* Boiss. are also found in the mountain
183 ranges of Southern Spain (Sierra de las Nieves and Grazalema).

184 Mountain vegetation (>1200 m asl) often presents continuous arboreal cover as, over the last
185 decades, forest recovery in previously managed montane regions has produced denser forest
186 communities. Yet, these montane-subalpine regions also host patchy plant communities where
187 forests blend with open ecosystems. Some species of juniper (*J. phoenicea* and *J. thurifera*) as
188 well as mountain and Scots pine (*P. sylvestris*, *P. uncinata* Ramond ex DC. in Lam. & DC.) are
189 present. This vegetation belt is also characterised by sparse scrub and grasses.

190 Cultivated olive trees (*Olea europaea* L.) are very extensive in the southern half of Spain (see
191 Fig. S1 in the Supplement), and often appear in the wild in shrubby habitat in the eastern half of
192 Spain. The olive tree is a key Mediterranean taxon that existed in Iberia before domestication,
193 represented since at least the Upper Pleistocene in continental records (i.e., Fernández et al., 2007;
194 González-Sampériz et al., 2020) and even the Early Pleistocene in the marine cores of Portugal
195 and Spain (Magri et al., 2017), but started to expand during the Early Holocene (Langgut et al.,
196 2019), with cultivation beginning during the late Middle Holocene and intensifying during the
197 last 4000 years (Carrión et al., 2010; Martín-Puertas et al., 2008).



198

199 Figure 2. Main forest types in the Iberian Peninsula (MITECO, 2024). Black dots represent the locations of the surface
200 samples used; red squares represent the coretops used for validation.

201

202 *b) Eurosiberian region*

203 The Eurosiberian or Atlantic region lies in the northern area of the STI, including the Cantabrian
204 range and the Pyrenees. Climatic conditions are characterised by cold winters and mild summers,
205 with MAT ranging from 5°C in the mountainous areas to 14°C in the coastal areas (Fig. 1).
206 Drought periods are shorter with abundant and well-distributed rainfall throughout the year, with
207 MAP ranging from 1000mm to 2000mm.

208 Forest composition differs considerably from that of the Mediterranean region. In coastal areas
209 (0-300 m asl), vegetation has been severely affected by invasive alien species (“Non-native
210 species communities” group in Fig. 2), especially by *Pinus radiata* D. Don and *Eucalyptus* spp.
211 L'Hér., both of which were cultivated for reforestation and industrial timber production but are
212 now naturalised. Forests dominate in montane areas (300-1000 m asl in the Cantabrian range;
213 1000-1600 m asl in the Pyrenees). These forests are deciduous or semi-deciduous mixed
214 communities of oaks (*Q. robur* L., *Q. petraea* (Matt.) Liebl., *Q. pyrenaica*), beech (*Fagus*
215 *sylvatica* L.), birch (*Betula alba*, *B. pendula*), ash (*Fraxinus angustifolia*, *F. excelsior*), hazel
216 (*Corylus avellana* L.) and other mesic taxa (“Mixed broadleaf communities group in Fig. 2) that
217 rarely form monospecific communities (*Sorbus aria* (L.) Crantz, *S. aucuparia* L., *Acer*
218 *monspesulanum* L., *A. opalus* Mill., *A. campestre* L., *Tilia cordata* Mill., *T. platyphyllus* Scop.,
219 *Juglans nigra* L., *J. regia* L., *Castanea sativa* Mill.). Atlantic mountains support conifers such
220 as *Pinus sylvestris* or *P. uncinata* (Fig. 2), or other conifers such as *Abies alba* Mill. (silver fir),
221 which often form mixed forests with beech in the Pyrenees (Fig. 2). Subalpine vegetation (1600-
222 2400 m asl) is characterised by sparse scrub and grasses, which are heavily grazed by livestock,
223 although conifers such as Scots and mountain pines can still be present, as well as the silver fir.
224 Mountain pine marks the alpine tree line (>2400 m asl), above which only grasslands and cushion
225 plant communities can resist the severe climatic stress found at these altitudes.

226 **2.2. Quantitative pollen-vegetation relationships**

227 *Brief overview of existing methods and why they are unsuitable for our study area*

228 Pollen-vegetation models have expanded over the last decades from those based solely on
229 pollen/vegetation ratios (Davis, 1963), linear regressions and extended R-values (ERV) (Parsons
230 and Prentice, 1981; Prentice and Parsons, 1983; Sugita, 1994), to the Landscape Reconstruction
231 Algorithm (Sugita et al., 2010) and the most recent Bayesian models (Dawson et al., 2016; Garreta
232 et al., 2012; Liu et al., 2022; Veeken et al., 2022).

233 One of the first attempts to develop appropriate techniques that account for pollen productivity
234 and dispersal was made by Davis (1963): the R-value model. This model assumes that pollen
235 deposition rates are directly proportional to abundances, each taxon having a characteristic
236 constant of proportionality, i.e., an R-value (Prentice and Parsons, 1983). The R-value would
237 designate the ratio between pollen percentage and vegetation percentage for each taxon. Parsons
238 and Prentice (1981) developed the Extended R-value (ERV) method, introducing two submodels
239 (ERV-1 and 2) to overcome the statistical limitations of ratios, site-to-site variability, and the
240 effects of long-distance pollen transport. ERV-1 expressed the background component (non-local
241 pollen) as “a constant background pollen percentage for each taxon” while ERV-2 expressed it as
242 “a constant proportion of total forest volume (or whatever measure of abundance is being used)”.
243 A third submodel (ERV-3) assumes a constant absolute amount of background pollen deposition
244 for each taxon at all sites (Sugita, 1994), since the correlation between pollen and vegetation will
245 not improve further beyond a certain distance, introducing the concept of the Relevant Source
246 Area of Pollen (RSAP). As a modification to ERV-3 to address site-to-site taxon variability,
247 (Theuerkauf and Couwenberg, 2022) developed ERV-4, expressing the background component
248 as a result of the pollen productivity multiplied by the distance-weighted regional plant abundance
249 for each taxon. ERV-1 and 2 use pollen and vegetation percentages, whereas ERV-3 and 4 use
250 pollen percentages and plant abundance data expressed in absolute abundances.

251 Sugita (2007a, 2007b) proposed a new framework for vegetation reconstruction, the Landscape
252 Reconstruction Algorithm (LRA), consisting of two different steps: the REVEALS and LOVE
253 models. The REVEALS (REgional VEgetation Estimates from Large Sites) model is designed to
254 reconstruct regional vegetation composition over large spatial scales (typically $>10^6$ hectares) by
255 correcting for biases in pollen representation due to differences in pollen productivity and
256 dispersal. It uses pollen data from large lakes or multiple small sites to estimate the relative
257 abundance of plant taxa in the surrounding landscape. This approach accounts for differential
258 pollen production and transport, making it more robust than simple pollen percentage analyses.
259 LOVE (LOcal VEgetation Estimates), on the other hand, focuses on reconstructing vegetation at
260 smaller spatial scales ($<10^4$ hectares) integrating regional vegetation estimates from REVEALS
261 with local pollen data to separate local vegetation signals from regional background. This two-
262 step framework allows for a hierarchical understanding of vegetation patterns, from broad
263 regional trends to fine-scale local dynamics.

264 More recently, pollen-vegetation models have been parameterised by using Bayesian hierarchical
265 models, which have the primary goal of accounting for the uncertainty of pollen dispersal and
266 production (Dawson et al., 2016; Liu et al., 2022; Paciorek and McLachlan, 2009). These
267 Bayesian approaches, contrary to the ERV, REVEALS and LOVE models, simultaneously
268 estimate pollen productivity and dispersal by finding the parameter values that best explain the
269 sediment pollen data given the known vegetation cover, adapting better to spatial complexity and
270 making them more suitable for regions with diverse vegetation and topography. However,
271 Bayesian approaches to estimating pollen productivity and dispersal are challenging to apply in

272 regions devoid of nearly-continuous sampling strategies (Dawson et al., 2016; Liu et al., 2022;
273 Trachsel et al., 2020). These models, as those from the ERV, typically assume relatively
274 homogeneous forest structure, consistent vegetation composition, and access to fine-scale,
275 spatially resolved vegetation data -conditions that are rarely met in complex landscapes like the
276 Iberian Peninsula-. In Iberia, vegetation is highly patchy and spans distinct bioclimatic zones, and
277 available data sources vary in resolution and taxonomic detail, making it difficult to replicate the
278 fine-scale separation between local and regional vegetation required by such models.
279 Additionally, the small size and topographic complexity of most Iberian lakes, along with the
280 presence of unique taxa with distinct dispersal traits, further complicate the direct application of
281 these Bayesian methods. In short, these particularities limit the transferability of the standard
282 Bayesian framework and highlight the need for regional recalibrations.

283 *Our methodological approach to compute RPPs in the Iberian Peninsula*

284 In this study, we have obtained RPPs relative to Poaceae by using a methodological algorithm
285 that finds optimal values (Fig. 3). Previous studies have already used iterative methods (Fang et
286 al., 2019) and global optimisation algorithms such as DEoptim (Mullen et al., 2011) to estimate
287 RPPs (Kuneš et al., 2019; Theuerkauf and Couwenberg, 2018) or pollen deposition parameters
288 (Theuerkauf and Couwenberg, 2017). Our approach builds upon previous work developed by
289 Kuneš et al. (2019) and using the 'disqover' R package (Theuerkauf et al., 2016).

290 We applied an algorithm that begins by generating initial candidate RPP values for each taxon,
291 which are then used to compute REVEALS estimates from pollen and vegetation data. The
292 distance between the REVEALS estimates and the observed vegetation is then calculated with a
293 loss function (eq. 1). To identify the best-fitting RPP values, we iteratively adjusted them to
294 minimise the loss function, using the Generalised Simulated Annealing algorithm, as
295 implemented in the GenSA package in R (Xiang et al., 2013) (Fig. 3). GenSA has not been
296 previously used in RPPs computation, and it belongs to a class of stochastic global optimisation
297 techniques particularly well-suited for navigating complex, multidimensional parameter spaces
298 characterised by numerous local minima. Unlike traditional optimisation approaches that may
299 become trapped in suboptimal solutions, Generalised Simulated Annealing leverages probabilistic
300 transitions to explore the solution space more broadly and escape local optima. GenSA is
301 implemented with a C++ core, ensuring computational efficiency and scalability for large
302 ecological datasets.

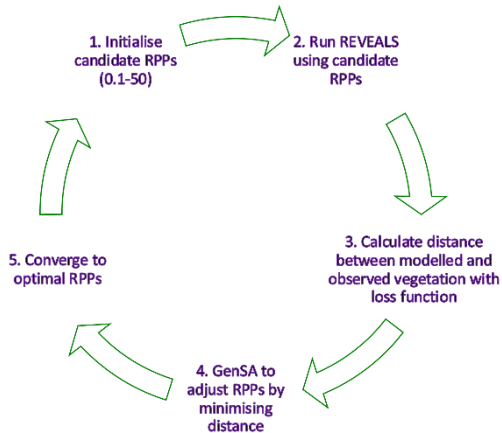


Figure 3. The optimisation loop to obtain RPPs. The algorithm starts with trial RPPs for each taxon (1). Uses candidate RPPs to estimate REVEALS from pollen data (2), and calculates distance between modelled and observed vegetation with a loss function (3). By using GenSA, the algorithm iteratively adjusts RPPs to minimise the loss function (4) until optimal RPPs are found (5).

319 GenSA identifies the optimal set of taxon-specific RPP values that minimises the discrepancy
 320 between observed regional vegetation composition and vegetation proportions reconstructed by
 321 the REVEALS model. The objective function minimised during optimisation is the weighted sum
 322 of squared errors (WSSE) between modelled and observed vegetation proportions across all
 323 regions. This approach aligns with the weighted least squares (WLS) regression (Carroll and
 324 Ruppert, 1988), although we included a smoothing offset in the denominator to reduce the
 325 influence of low-abundance taxa and to avoid division by zero:

$$326 \quad L(a) = \sum_{r=1}^R \sum_{i=1}^m \frac{(V_{i,r}^{mod} - V_{i,r}^{obs})^2}{V_{i,r}^{obs} + 1} \quad (1)$$

328 where:

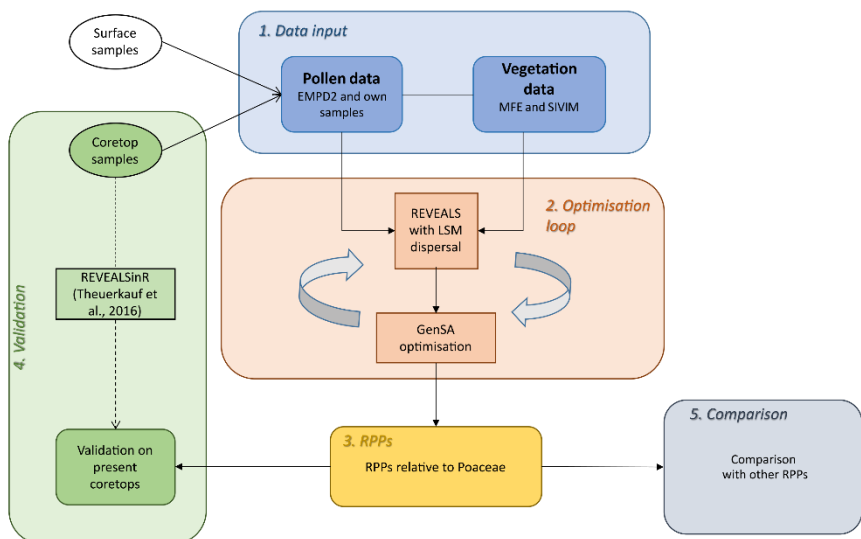
329 • a : vector of RPP to be estimated
 330 • R : number of analysed grids
 331 • m : number of taxa
 332 • $V_{i,r}^{mod}$: vegetation proportion for taxon i in region r , reconstructed by REVEALS
 333 • $V_{i,r}^{obs}$: observed vegetation proportion of taxon i in region r .

334 Retrieving RPPs with the optimisation loop involved first setting the initial range of possible
 335 pollen productivity values to 0.1-50 (Fig. 3), meaning that the optimisation function would search
 336 for 500 possibilities before displaying the RPPs that gave the smallest distance between observed
 337 and reconstructed vegetation proportions. Moreover, we set 500 iterations to ensure the decrease
 338 between each run, and bootstrapped 100 resampled versions of all the sites, in order to obtain
 339 error estimates. Since such a setup of the parameters requires high computational efforts (500x100
 340 runs per taxon are needed to retrieve a single RPP), we compiled the optimisation function for a
 341 better performance by using the ‘compiler’ package, included in base R (R Core Team, 2025).
 342 We also parallelised the optimisation process using ‘foreach’ (Microsoft and Weston, 2009) and
 343 ‘doParallel’ (Microsoft and Weston, 2011) packages. Full code workflow is provided in the
 344 Supplement.

345 Regarding pollen dispersal, this parameter is crucial for reconstructing past vegetation
 346 abundances, although in practice it is not possible to reliably measure long-distance dispersal of

347 airborne particles (Katul et al., 2005). While models for predicting airborne particle dispersion
 348 are needed (Kuparinen et al., 2007), the correct model selection according to the studied area is
 349 also key. In the present work, we use the Lagrangian Stochastic model (LSM) (Andersen, 1991;
 350 Kuparinen et al., 2007) to calculate the dispersal and deposition factor, which allows better
 351 simulations of pollen dispersal over short and long distances than the Gaussian Plume model
 352 (GPM) (Jackson and Lyford, 1999), which fails to predict the magnitude of long-distance
 353 dispersal (Kuparinen, 2006; Mariani et al., 2016; Theuerkauf et al., 2016).

354 In short, we have developed a framework that could be applied in other regions, in which we use
 355 the inverted (Theuerkauf, 2025) or reverse REVEALS approach, i.e., we estimate REVEALS
 356 before calculating RPPs, then validated the results using modern coretop samples and compared
 357 them with other pollen productivity estimates from Europe (Fig. 4).



358

359 Figure 4. Methodological workflow of this study. Pollen data (from surface and coretop samples) and vegetation data
 360 were used (1) to calculate present-day REVEALS estimates. Using a Lagrangian stochastic dispersal model, the GenSA
 361 optimisation algorithm was applied (2) to identify the optimal set of RPPs relative to Poaceae, minimising the difference
 362 between observed and REVEALS-estimated vegetation proportions (3). The resulting RPPs were validated against
 363 present-day coretops (4) and compared with values obtained in other studies (5), following the numerical pipeline
 364 described in Abraham and Fořtová (in prep.) and Sect. 2.3. “RPPs comparison across European studies”.

365 2.2.1 Pollen and vegetation data acquisition

366 The taxa chosen for RPPs computations include the most frequent arboreal types in both present-
 367 day STI forests and palynological sequences (Carrión et al., 2022) to which we can attribute pollen
 368 types: *Abies* Mill., *Betula* L., *Corylus* L., *Fagus* L., *Pinus* L., *Olea* L., deciduous and evergreen
 369 *Quercus* L. Shrub and herbaceous taxa from frequently represented families and genera in STI
 370 vegetation and fossil pollen records have also been included: Amaranthaceae/Chenopodiaceae
 371 Juss., *Artemisia* L., Asteraceae. SF. Asteroideae Lindl., Brassicaceae Burnett, Asteraceae. SF.
 372 Cichorioideae Chevall., *Erica* L., *Genista*-type (*Genista* L. and *Ulex* L.), *Juniperus* L., *Plantago*
 373 L., Poaceae Juss., Ranunculaceae Juss., Rosaceae Juss. and *Rumex* L.

374

375

376

377 *Pollen data*

378 Producing the necessary RPPs for STI requires analysis of a large number of sampling points of
379 both modern pollen and vegetation cover. Therefore, we divided the study area into 25 grids of
380 150x150 km² each (Fig. S2 in the Supplement). The percentage of pollen for the main taxa was
381 then retrieved for each grid, and compared with regional vegetation data.

382 We used modern pollen counts from the Eurasian Modern Pollen Database 2 (hereafter referred
383 to as EMPD2) (Davis et al., 2020). According to the EMPD2, the region of continental Spain has
384 the second highest number of samples, with 1,110 modern pollen samples taken from terrestrial
385 moss pollsters, soils or lake sediments.

386 We reviewed the sample context and excluded those originating from marine and estuarine
387 environments, resulting in the selection of 1,113 samples, of which 70 were obtained through our
388 own field surveys, conducted at various times over the past 30 years. Pollen productivity estimates
389 were then obtained by excluding 51 modern coretops from open areas that have been used as a
390 validation set (see Fig. 4 and Sect. 2.2.2. “Validation of RPPs”). Pollen fall speed was retrieved
391 from literature (Tables S1 and S2, Supplement) or calculated following Stoke’s law for spherical
392 particles and Falck’s assumption for ellipsoidal grains (Gregory, 1961) with the photographs
393 contained in reference collections (Reille, 1992, 1995).

394 *Vegetation data*

395 Present-day arboreal vegetation cover for the 150 x 150 km² grids was obtained through the most
396 recently published database of the Spanish Forestry Map (MFE) at a scale of 1:25000 (MITECO,
397 2024). MFE classifies the vegetation cover into plant communities for which detailed information
398 on the coverage of the 3 main woody, arboreal or shrub species is provided. We then estimated
399 the forest patch size by multiplying the percentage cover of each main species by the area of the
400 polygon in which it is located.

401 For shrub and herbaceous taxa we used the *relevé*-based database Information System on Iberian
402 and Macaronesian Vegetation (SIVIM) (Font et al., 2017). We used all the available plant
403 inventories from SIVIM, using a total of 149,646 surveys where we performed taxa harmonisation
404 according to pollen types (Tables S1 and S2, Supplement).

405 We derived information on crops and other land uses using the CORINE land cover (CLC)
406 database (European Environment Agency, 2019) so all vegetation types could be analysed,
407 especially in areas where human-modified landscapes are dominant. We spatially intersected CLC
408 polygons with MFE to classify each territory unit according to both land use type and forest cover
409 presence/absence. This dual classification differentiates between areas designated as forest by
410 CLC that indeed retain actual forest cover and those that have undergone deforestation. The
411 resulting landscape matrix was then combined with SIVIM data, which incorporates shrub and
412 herb taxa, to quantify the floristic composition across different landscape contexts and forest
413 cover conditions. Additionally, CLC provided critical information on *Olea europaea* crop
414 abundance, which is absent from MFE as olive typically represents agricultural rather than natural
415 forest systems.

416 **2.2.2. Validation of RPPs**

417 Validating REVEALS-based vegetation estimates using modern forest composition and raw
418 pollen data requires an independent dataset. Accordingly, we excluded 51 coretop samples from
419 the EMPD2 dataset when deriving RPPs (Fig. 4). This allowed us to reconstruct vegetation
420 proportions for those sites using our new RPPs, and compare them with actual forest cover. From
421 the 51 coretops validation dataset we chose 26 samples by excluding salt lakes, where the surface

422 samples are often subject to aeolian erosion, and samples under closed canopy or from high
423 elevations where the pollen signal might be biased.

424 We validated RPPs on those 26 samples using the REVEALSinR function from the ‘disqover’
425 package (Theuerkauf et al., 2016) to account for the productivity and dispersal-deposition biases.
426 Data input requires: i) pollen counts at each lake site from which the coretop comes; ii) estimates
427 of pollen productivity and fall speed of pollen for all taxa; iii) standard errors of the RPPs; iv)
428 distance-weighting method, for which the LSM was selected; v) basin type (peatland or lake) and
429 diameter in meters for each and; vi) diameter of the reconstructed region in meters. REVEALSinR-
430 based estimates of the modern samples were then compared with rings of 15, 30, 45 and 100 km
431 of present tree cover around each sample. Only arboreal taxa were selected, since herb and shrub
432 taxa data are devoid of surface area information. Regional plant cover for validation was obtained
433 from the MFE, except for *Olea* (olive crops) which was calculated from the CORINE Land Cover
434 dataset.

435 Evaluation of the validation process was conducted using a multimetric approach based on four
436 error and bias metrics for each taxon: root mean square error (RMSE), mean absolute error
437 (MAE), mean absolute percentage error (MAPE) and normalised mean bias (NMB). RMSE and
438 MAE quantify absolute deviations, with RMSE emphasising larger errors, MAPE expresses
439 deviations relative to observed values, and NMB captures systematic over- or underestimation.
440 Each metric was calculated as the difference between raw pollen estimates and REVEALSinR-
441 derived values, standardised using z-scores, and averaged per taxon to produce a composite
442 improvement score—a dimensionless measure of validation performance.

443 Given the large volume of validation results, this paper focuses on the coretop validation at 45
444 km resolution, which showed the strongest performance according to the multimetric analysis.
445 The rest of the results regarding the validation can be found in the Supplement (Fig. S3-S5).

446 **2.3. RPPs comparison across European studies**

447 Comparing RPPs between studies has become a challenging task due to the large number of
448 existing studies all making partially different assumptions. Recently, Abraham and Fořtová (in
449 prep.) introduced a numerical pipeline designed to address such a challenge, enabling more
450 reliable comparisons by correcting biases in original studies (e.g., use of incorrect dispersal
451 models) and resolving methodological discrepancies between studies (e.g., different reference
452 taxa).

453 We applied this pipeline to compare RPPs from published studies across Europe with our new
454 dataset (Fig. 3), implementing the following steps:

- 455 1. Debiasing RPPs for heavy pollen grain taxa: we corrected the RPP value for *Abies*
456 according to Theuerkauf (2025), as the original estimate was based on an inappropriate
457 dispersal model (Gaussian Plume Model).
- 458 2. Taxon ratio comparison: we calculated ratios between pairs of taxa in our dataset and
459 compared them to corresponding ratios in previous studies. A taxon pair from a previous
460 study was considered matching if its ratio differed by no more than a factor of 1.5 (i.e.,
461 within the range of 0.67 to 1.5) from the equivalent ratio in our dataset.
- 462 3. Selection criteria: the number of matching taxon pairs and the number of individual taxa
463 involved in those matches were used to identify studies suitable for further comparison.
464 In this study, RPPs from *Erica* and *Genista*-type were compared to RPPs of Ericaceae
465 and Fabaceae, respectively.
- 466 4. Removing effect of reference taxon: in our dataset, Poaceae was used as the reference
467 taxon and assigned a RPP value of 1. To standardise other studies, we used matching taxa
468 in common and averaged their differences to scale RPP values accordingly.

469 5. Visualisation: for selected studies, we visualised the RPPs of comparable taxa using two
470 approaches:

471 a. Standard bar plots with axes ranging from 0 to the maximum RPP value.
472 b. Fold-change symmetric bar plots, where values <1 were plotted below the
473 horizontal axis as reciprocals (e.g., a RPP of 0.1 is shown as 1/10 below the axis),
474 and values >1 were plotted above. This approach allows for multiplicative
475 inverse of RPPs.

476 Previous RPP studies often include multiple sets of pollen samples, analysed using different
477 methods. For each original study conducted in Europe, we selected one representative set of RPP
478 values corresponding to a distinct set of pollen samples. Regarding the calculation methods (e.g.,
479 the ERV models), we followed choices outlined by Githumbi et al. (2022). However, the RPPs
480 themselves were sourced from Wieczorek and Herzschuh (2020), who provided the original,
481 unmodified estimates without recalculation. References of the studies used for comparison are
482 available in Table 1.

483 Table 1. List of studies included in the comparison. Full metadata of the references are available in Table S3 in the
484 Supplement.

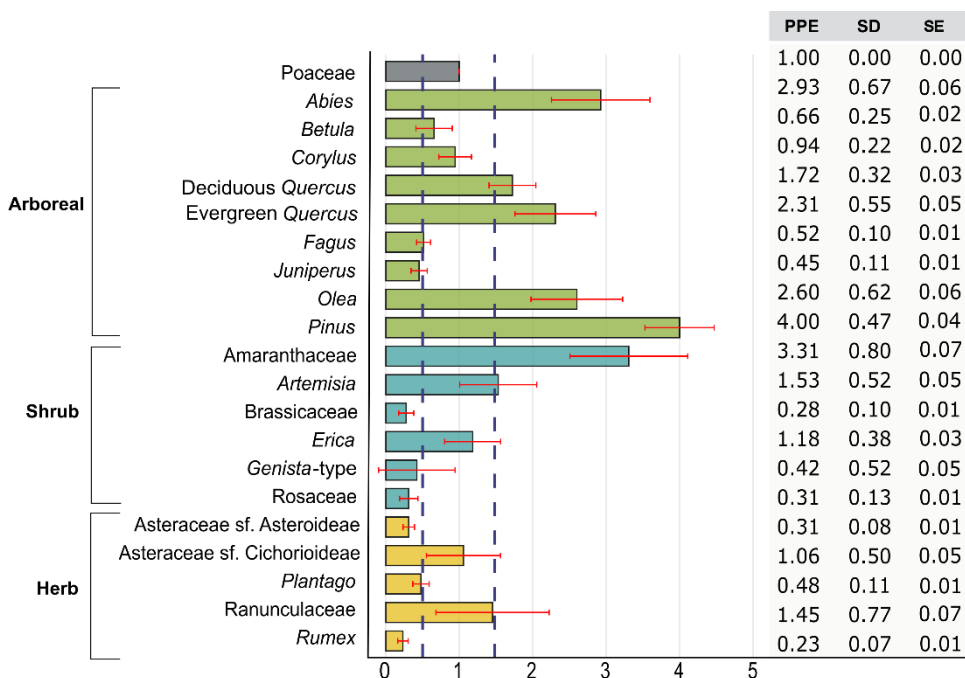
Code	Reference	Country	Region
A	Bunting et al., 2005	England	Calthorpe
B	Bunting et al., 2005	England	Wheatfen
C	Räsänen et al., 2007	Finland	North
D	Theuerkauf et al., 2013	Germany	Northeast (i)
E	Theuerkauf et al., 2013	Germany	Northeast (ii)
F	Twiddle et al. 2012	Scotland	East
G	Von Stedingk et al., 2008	Sweden	West and central
H	Baker et al., 2016	Poland	Poland
I	Andersen, 1970	Denmark	South
J	Hjelle, 1998	Norway	Inland
K	Matthias et al., 2012	Germany	East
L	Nielsen, 2004	Denmark	Denmark
M	Poska et al., 2011	Estonia	Southeast
N	Broström et al., 2004	Sweden	South (i)
O	Hjelle, 1998	Norway	Coast
P	Abraham and Fořtová (in prep.)	Czech Republic	West
Q	Abraham et al., 2014	Czech Republic	Czech Republic
R	Theuerkauf et al., 2015	Germany	Northeast
S	Soepboer et al., 2007	Switzerland	Swiss Plateau
T	Sugita et al., 1999	Sweden	South (ii)
U	Mazier et al., 2008	Switzerland	Jura Mountains
V	Mazier (unpubl.) in Githumbi et al. (2022)	France	South
W	Abraham and Kozáková, 2012	Czech Republic	Central
X	Hjelle and Sugita, 2012	Norway	South

Y	Kunes et al., 2019	Czech Republic/Slovakia	White Carpathians
Z	Grin Dean et al., 2019	Romania	Southeast

485

486 **3. Results**487 **3.1. Pollen productivity estimates**

488 The first RPPs relative to Poaceae in STI identify low, medium and high pollen producers (Fig. 489 5). Low pollen producers (lower than 0.48) are Asteraceae sf. Asteroideae, Brassicaceae, *Genista*-490 type, *Juniperus*, *Plantago*, Rosaceae and *Rumex*; medium producers (0.49-1.42) are *Betula*, 491 Asteraceae sf. Cichorioideae, *Corylus*, *Erica*, *Fagus* and Ranunculaceae, while high producers 492 (>1.43) are *Abies*, *Artemisia*, Amaranthaceae, *Olea*, *Pinus*, evergreen and deciduous *Quercus*.



493

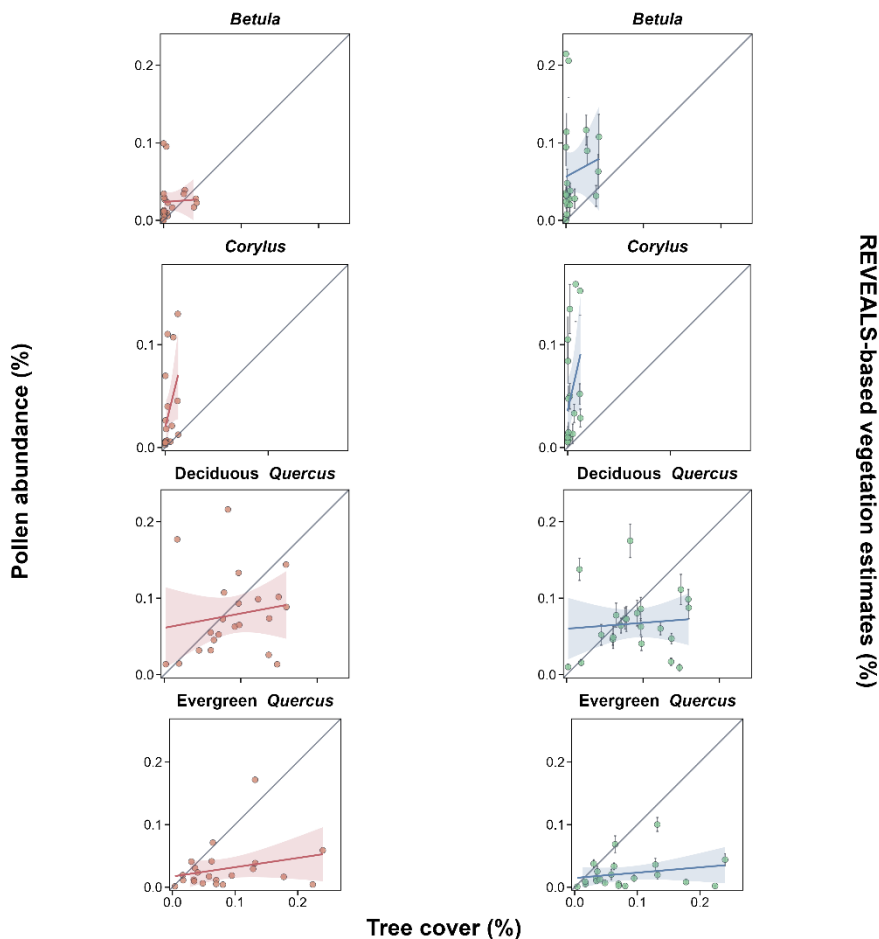
494 Figure 5. Relative pollen productivity estimates (RPPs) relative to Poaceae with standard deviation (SD) 495 and standard error (SE) for 21 characteristic taxa in continental Spain. Red bars refer to the SD. Blue 496 dashed lines indicate the cutoff values, based on percentiles, between low, medium and high pollen 497 producers. Colours refer to the different groups of taxa (Poaceae in grey, arboreal in green, shrubs in teal and herbs in yellow).

498 The calculated RPPs for continental Spain are publicly available at 499 <https://doi.org/10.5281/zenodo.17927544> (Jungkeit-Milla et al., 2025).

500 **3.2. Validation of RPPs on modern coretops**

501 RPPs relative to Poaceae for 8 arboreal taxa (all arboreal taxa considered in this study except for 502 *Abies* because it is not present in the whole STI and therefore lacking in most coretop samples) 503 were applied to 26 coretops to test their robustness (Fig. 6).

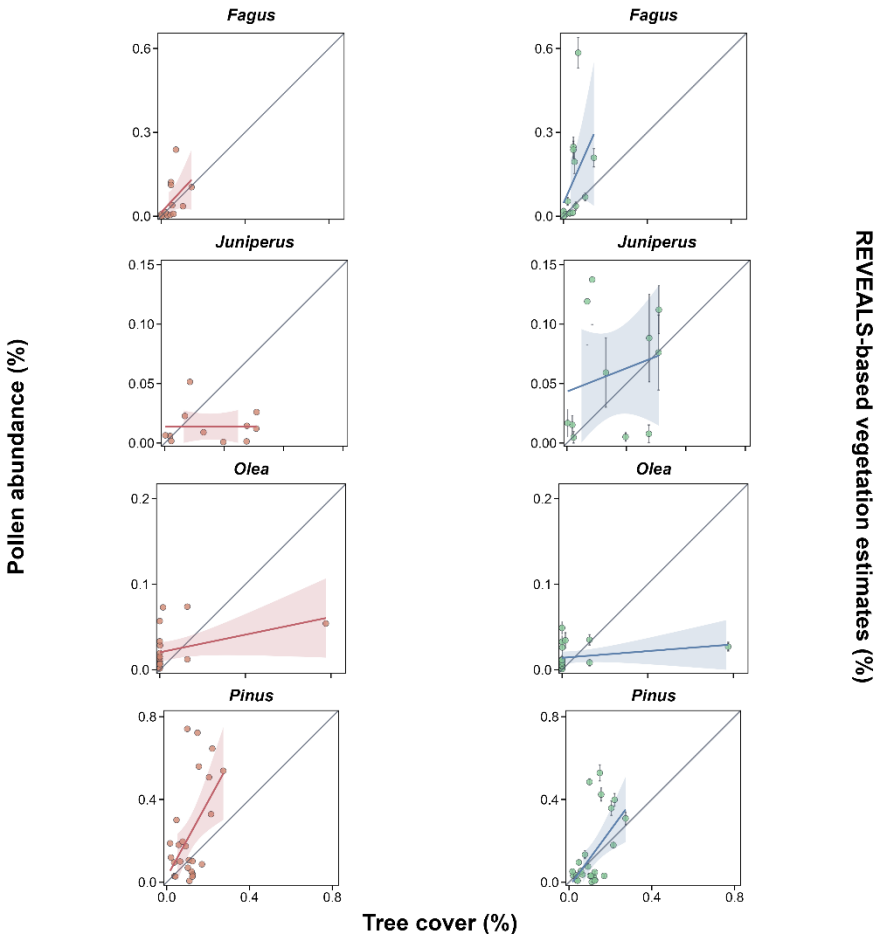
504 The REVEALS model attempts to correct the uneven pollen productivity across taxa, resulting in
 505 an abundance reduction of overrepresented taxa and an increase for the underrepresented taxa
 506 (Fig. 6). This correction is evident when comparing raw pollen percentages (Fig 6, left column)
 507 with REVEALS-based vegetation estimates (Fig 6, right column). *Pinus* and both evergreen and
 508 deciduous *Quercus*, which dominate Iberian tree communities, show a marked reduction in
 509 estimated vegetation cover. The case of *Pinus* is especially illustrative: the adjusted estimates
 510 align closely with the observed vegetation cover (Fig. 6), suggesting the model performs well in
 511 accounting for its high pollen productivity. Another important example is *Olea*, for which
 512 REVEALS estimates indicate a reduction in the extent of olive cultivation. Nonetheless, several
 513 coretops were found to have no crops within a 45 km radius and we found that pollen from *Olea*
 514 correlated better with olive crop coverage at 100 km distance (see Fig. S3, S4 and S4 in the
 515 Supplement).



516 Figure 6. Relationship between the mean tree cover at 45km in each coretop with untransformed pollen abundances
 517 (left, in red) and with the REVEALS-based vegetation estimates (right, in blue) with standard errors. The grey diagonal
 518 line represents the 1:1 reference line, indicating perfect correspondence between pollen/vegetation estimates and actual
 519 tree cover. Coloured lines represent linear regressions with 95% confidence intervals (shaded areas). Points above the
 520 reference line suggest pollen overrepresentation relative to actual tree cover, while points below indicate
 521 underrepresentation.

522

523



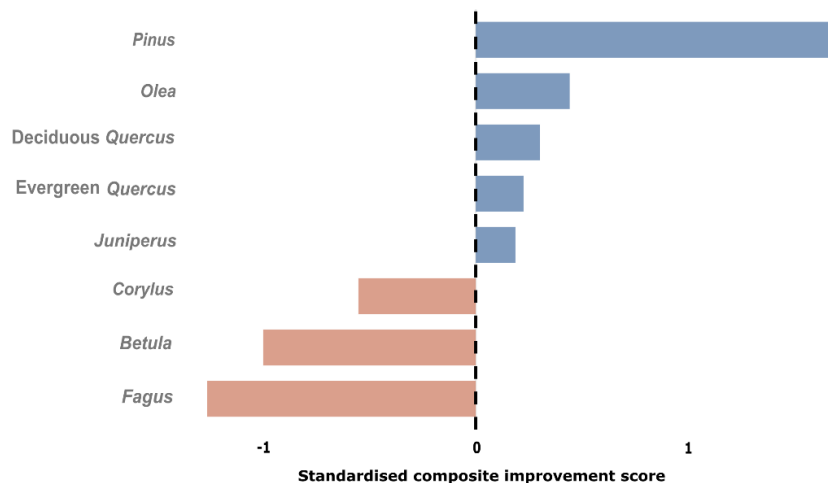
524 Figure 6. Continued.

525 On the contrary, temperate forest taxa such as *Betula*, *Corylus* and *Fagus*, having relatively low
 526 RPPs (Fig. 5), tend to be underrepresented in pollen assemblages in Iberia. REVEALS corrects
 527 for this bias, resulting in higher vegetation estimates for these taxa. *Juniperus*, moderately
 528 underrepresented in raw pollen data likely due to low pollen productivity (Fig. 5), is partially
 529 corrected by REVEALS, resulting in slightly higher estimates of vegetation cover. The
 530 standardised composite improvement score of the multimetric analysis at 45 km revealed that
 531 temperate forest taxa perform better with raw pollen counts than with the REVEALS-based
 532 reconstructions when comparing with observed regional vegetation cover (Fig. 7). Nonetheless,
 533 REVEALS estimates still provide more ecological sense in accounting for the observed
 534 vegetation than pollen percentages for *Betula* at 15 km and 100 km (Fig. S3 and S5 in the
 535 Supplement).

536

537

REVEALS-based vegetation estimates (%)



538 Figure 7. Multimetric analysis comparing performance of REVEALS at 45 km for the selected arboreal taxa.

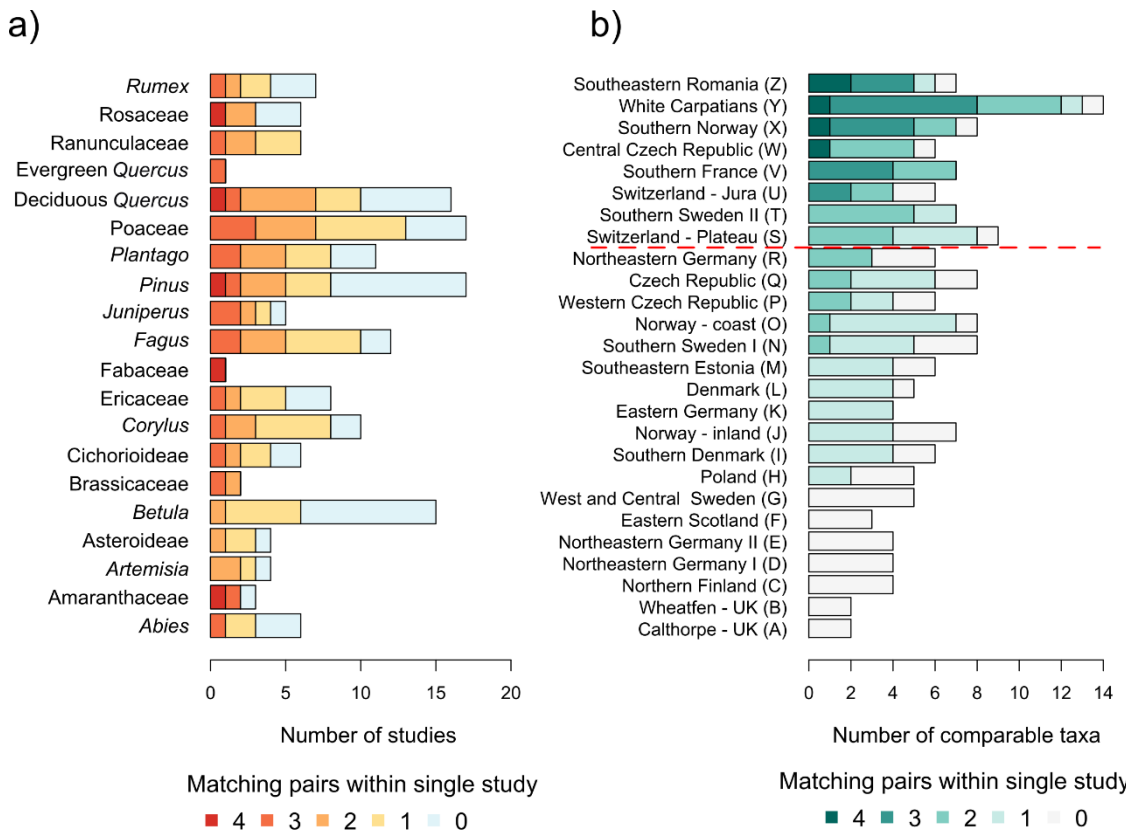
539

540 **3.3. RPPs comparison across European studies**

541 Comparison of RPPs demonstrated similar values, at least in one pair, in all or more than half of
 542 the previously published values for the following taxa: Amaranthaceae, *Artemisia*, Asteraceae sf.
 543 Asteroideae, Brassicaceae, Asteraceae sf. Cichorioideae, *Corylus*, Ericaceae (*Erica*), Fabaceae
 544 (*Genista*-type), *Fagus*, *Juniperus*, *Plantago*, Poaceae, evergreen and deciduous *Quercus*,
 545 Ranunculaceae and *Rumex*. In contrast, the remaining taxa – *Abies*, *Betula*, *Pinus* and Rosaceae -
 546 , show agreement with only half or fewer of the European sites (Fig. 8a).

547 The eight studies with the highest number of matching taxa are from France, Switzerland, Czech
 548 Republic-Slovakia, Romania, Norway, and Sweden. The remaining studies, which show lower
 549 similarity between RPPs, come from Great Britain, Germany, Denmark, Poland, Estonia, and
 550 Finland (Fig. 8b).

551



552

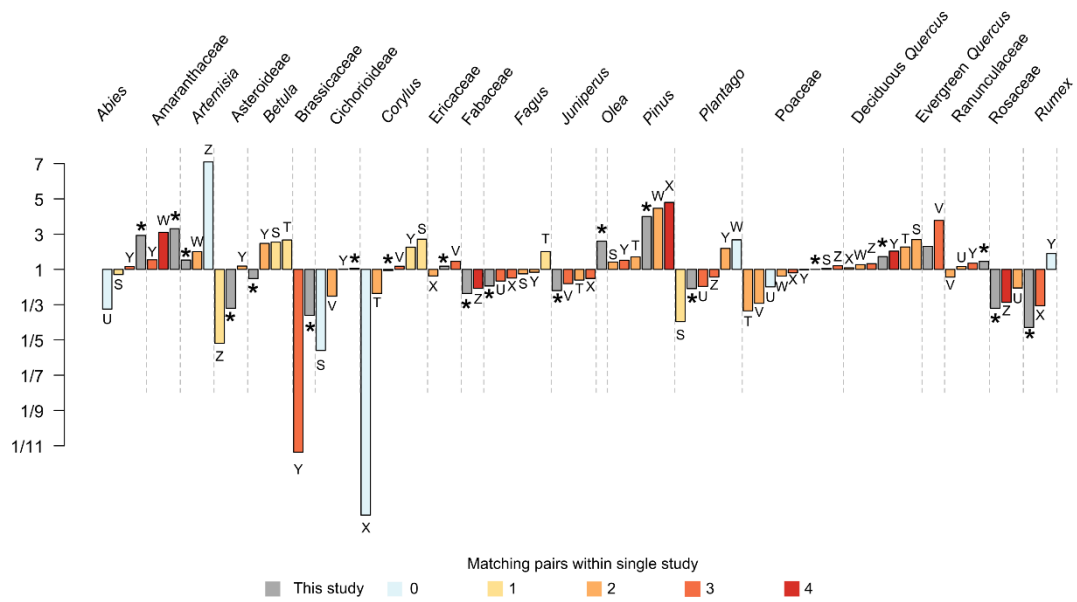
553 Figure 8. Number of RPP studies across Europe per taxon (a) and number of comparable taxa per study across Europe
554 (b). Darker colours indicate species appearing in matching pairs of species. Each letter in (b) represents a different
555 studied region (see Table 1 for details of the country for each study). Dashed red line in (b) indicates the similarity
556 threshold.

557

558 For several taxa—*Quercus* (deciduous), Asteraceae sf. *Astroideae*, *Corylus*, Ericaceae,
559 *Plantago*, Poaceae, and *Pinus*—the STI RPPs are near the midpoint of the observed range in
560 similar studies (Fig. 9). Notably, Poaceae and *Pinus* form two distinct clusters across studies; the
561 STI values are within the higher cluster (4 for *Pinus*, and 1 for Poaceae).

562 For the remaining taxa, STI RPPs are distributed towards the edges of the observed ranges (Fig.
563 9), though still close to some previously reported values. These include Amaranthaceae,
564 *Artemisia*, Asteraceae sf. Cichorioideae, Fabaceae, *Fagus*, *Juniperus*, Ranunculaceae, and
565 Rosaceae. In the case of *Abies*, our estimate is higher than from any other European studies, while
566 for *Betula* and *Rumex*, the values are lower.

567 Only two studies have derived RPPs for Brassicaceae, Fabaceae and evergreen *Quercus*, while
568 only the present study provides a RPP for *Olea*. Within this limited data, *Quercus* evergreen is
569 consistently represented as a high pollen producer, whereas Brassicaceae appears as a low pollen
570 producer (Fig. 9).



571

572 Figure 9. Fold-change symmetric barplot of recalculated RPPs from the eight most similar studies. Adjustments
 573 account for reference taxon differences and dispersal model correction for *Abies*. Values <1 plotted as reciprocals.
 574 Each bar represents one of the eight most similar studies (letters S-Z), coming from Swiss Plateau (S), Southern
 575 Sweden (T), Jura Mountains in Switzerland (U), Southern France (V), Central Bohemia in Czech Republic (W),
 576 Southern Norway (X), White Carpathians (Y) and Southeastern Romania (Z). Asterisk (*) refers to the values of this
 577 study. See Table 1 for more details of each study. See Fig. S6 in the Supplement for RPPs with confidence intervals.

578 4. Discussion

579 The results presented here are the first RPPs produced in Iberia. Our results show clear differences
 580 in pollen productivity among the 21 taxa analysed. Among the low producers, herbaceous and
 581 shrub taxa dominate, while the medium and high pollen producers include a mix of trees and
 582 shrubs. Validation using coretops indicated that RPPs of the dominant taxa in present-day
 583 landscapes are more accurately estimated than the less abundant ones. Comparison with
 584 previously published European RPPs shows that our estimates align closely with 8 different
 585 studies. Our discussion is thus framed around our three main objectives of estimating, evaluating
 586 and comparing the Iberian RPPs under the prism of the methodological challenges we found.

587 Validation and potential implementation of the first Iberian pollen productivities

588 The validation presented in this study is the first carried out in heterogeneous environments of the
 589 Western Mediterranean using vegetation survey data and disaggregated by taxa rather than by
 590 total tree cover. Validation of RPPs in modern samples remains uncommon but has been
 591 performed for all Europe (Serge et al., 2023), southern Sweden (Hellman et al., 2008), Australia
 592 (Mariani et al., 2017, 2022) and various Asian regions (Jiang et al., 2020; Wan et al., 2022; Xu et
 593 al., 2014). They generally found an excellent performance for large groups of taxa, although the
 594 fit between the modelled estimates and the vegetation data was not always as good when single
 595 taxa were considered (Hellman et al., 2008). Wan et al. (2022) presented the first evaluation of
 596 RPPs in a tropical region, suggesting that the REVEALS model performs well especially when
 597 applied at the landscape level rather than for individual species. In our dataset, we could not
 598 validate REVEALS for herb and shrub taxa because MFE only includes arboreal taxa.
 599 Nevertheless, our hypothesis is that some herb and shrub taxa would be overrepresented if we
 600 apply REVEALS, as in Li et al. (2023) or in Marquer et al. (2020), since in Iberia these are low
 601 pollen producers, as it happens with other trees as *Betula*, *Corylus* and *Fagus*.

602 REVEALS generally performed well when reconstructing the coverage of arboreal taxa (Fig. 6),
603 although only 5 of the 8 taxa performed better with REVEALS than with pollen abundances,
604 according to the multimetric analysis performed at 45 km radius: *Pinus*, *Juniperus*, *Olea*,
605 deciduous and evergreen *Quercus* (Fig. 7). *Juniperus* showed improved performance as the
606 distance increased, specifically up to 45 km (see multimetric results at other distances in the
607 Supplement), likely because junipers occur in small coves or patchy forest stands, so the greater
608 the distance considered, the more individuals are found. In this work, we calculated the first
609 pollen productivity estimate for *Olea*. We found that *Olea* is a high pollen producer, which was
610 to be expected considering its high dispersal capability (Cañellas-Boltà et al., 2009; Fernández-
611 Rodríguez et al., 2014) and its presence in modern samples where the nearest olive trees are more
612 than 70 km away (Leunda et al., 2017). In our modern samples, most of the *Olea* pollen comes
613 from olive crops in southern Spain. The MFE inventory rarely includes the olive tree, since it does
614 not form forests or small groves naturally. These two examples underscore the need of accounting
615 for source area when interpreting pollen records, particularly for taxa frequently employed as
616 indicators of environmental change. The contrasting distribution patterns and dispersal capacities
617 of *Juniperus* and *Olea* demonstrate how spatial context and distance exert a substantial influence
618 on pollen representation.

619 The standard errors of the 8 validated taxa were consistently lower than their estimates, providing
620 a measure of precision in terms of reliability (Githumbi et al., 2022; Li et al., 2023). Nevertheless,
621 the quality of REVEALS outputs is ultimately constrained by the quality of input datasets (EMP2
622 and MFE). According to the theory, deviation of REVEALS estimates from observed vegetation
623 may suggest unreliable RPP values. We however believe that such deviation could be explained
624 by: (i) a poor performance of REVEALS for *Betula*, *Corylus* and *Fagus*, since they are not present
625 in all the STI due to environmental heterogeneity; and (ii) inaccuracies in the vegetation dataset,
626 especially for taxa that do not form large, continuous forests such as *Juniperus*, *Betula* or *Corylus*
627 (Wan et al., 2022).

628 In light of our results, we believe that implementing our RPPs to quantitatively reconstruct
629 vegetation cover from fossil pollen records could be promising for both arboreal and non-arboreal
630 taxa in Iberia. The relatively low SEs for trees in our validated coretops (especially for *Pinus*,
631 *Olea* and both evergreen and deciduous *Quercus*) indicate that they can be confidently used for
632 regional reconstructions of past vegetation. Even for some less optimally performing taxa, such
633 as the temperate forest species, these RPPs can serve as a baseline until region-specific estimates
634 become available. As for shrub and herb taxa, while direct validation was not possible, the
635 generally robust SEs we retrieved suggest that these values could be cautiously implemented in
636 reconstructions of open vegetation dynamics within Mediterranean landscapes.

637 The overrepresentation of trees in pollen records aligns with findings from other European studies
638 and with long-lasting intuitive expectations in the palaeoecological community. Notably
639 significant are the values among dominant tree species: *Pinus* (4.00), evergreen (2.31), and
640 deciduous (1.72) *Quercus*, suggesting a lower prevalence of pine communities in the past than
641 has been interpreted based on previous reconstructions that indicated a higher abundance of pines,
642 using both pollen data and/or wood charcoal and macrofossil analyses (Aranbarri et al., 2014,
643 2020; Carrión et al., 2004; Ezquerra et al., 2019; Múgica et al., 2001; Rubiales et al., 2010).
644 Conversely, some deciduous trees in Iberia, such as *Betula* (0.66) and *Fagus* (0.52), showed lower
645 productivity, potentially leading to being underrepresented in fossil pollen records. This
646 underestimation could affect our understanding of Pleistocene and Holocene temperate forest
647 dynamics unless RPPs are applied (Broström et al., 2005; Githumbi et al., 2022; Trondman et al.,
648 2015). For instance *Corylus*, with a RPP near 1, provides crucial information for linking it to, e.g.,
649 early postglacial vegetation expansions (Aranbarri et al., 2014; González-Sampériz et al., 2006;

650 Pearce et al., 2025b; Theuerkauf et al., 2014), and post-disturbance responses (Gil-Romera et al.,
651 2014; Leunda et al., 2020).

652 For herb and shrub taxa with particularly low RPPs, such as *Rumex* (0.23), *Brassicaceae* (0.28),
653 *Juniperus* (0.45) or *Plantago* (0.48), their roles in vegetation dynamics are expected to be
654 underestimated if only raw pollen counts are considered in fossil records. This is especially
655 critical for taxa associated with anthropogenic activities, such as *Plantago* or *Rumex*, whose
656 historical presence in the Mediterranean landscape may be stronger than traditionally inferred
657 without REVEALS estimates (Grin Dean et al., 2019; Kuneš et al., 2019; Mazier et al., 2008;
658 Soepboer et al., 2007).

659 Our RPPs demonstrate that raw pollen assemblages may bias reconstructions of Pleistocene and
660 Holocene vegetation by overemphasising high pollen producers such as conifers and some oaks
661 while downplaying the ecological importance of low-productivity taxa, including several
662 deciduous broadleaved trees and herbs. Future quantitative reconstructions of vegetation
663 dynamics in the STI hold the potential to substantially advance debates on the contentious idea of
664 past continuous forest canopies in Iberia (Gomes et al., 2020; Pérez-Obiol et al., 2011).
665 Incorporating revised pollen productivity estimates may reveal an even more fragmented forest
666 landscape in the Southwestern Mediterranean, characterised by a mix of broadleaf woodlands,
667 coniferous patches, temperate forests and open areas, as has been previously suggested (i.e., see
668 compilations and references there in Carrión et al., 2010a and González-Sampériz et al., 2010).

669 Future implementations in Iberia expand the possibilities to reconstruct past disturbances. By
670 integrating RPPs into fossil pollen records, we can quantify vegetation composition over time and
671 estimate biomass dynamics affected by various disturbances. With reliable RPPs, it becomes
672 feasible to produce spatially explicit models showcasing the long-term effects of environmental
673 drivers across time and space, including anthropogenic or natural factors as well the long-term
674 interactions between disturbances and ecosystem recovery (Githumbi et al., 2022; Knight et al.,
675 2022; Theuerkauf and Couwenberg, 2017).

676 *Pollen productivities across Europe*

677 Dominant vegetation types of the STI - pines, evergreen and deciduous oaks - exhibited RPP
678 values successfully validated with independent top core samples. These taxa are identified as high
679 pollen producers, consistent with findings from previous studies, particularly after adjusting
680 original RPP values by the average scaling factor (see Sect. 2.3. “RPPs comparison across
681 European studies”). Specifically, *Pinus* showed a RPP of 4.0 (Fig. 9), which aligns reasonably
682 well with values reported from Central Czech Republic (4.5) and Southern Norway (4.8) (letters
683 W and X in Fig. 9, respectively). Evergreen *Quercus* exhibited a RPP of 2.31, comparable to 3.8
684 reported in Southern France (letter V, Fig. 9), and deciduous *Quercus* had a RPP of 1.72, which
685 closely matches the value of 2.0 from the White Carpathians (letter Y), in Czech Republic and
686 Slovakia.

687 We also observed that our RPPs for most taxa fall near the midpoint of the range observed in
688 other European studies, which is of interest since the STI has different environmental conditions
689 that could have influenced pollen productivity. High pollen producers include wind-pollinated
690 shrubs and herbs such as *Amaranthaceae* (3.31) and *Artemisia* (1.53), which yielded similar
691 values to those reported in the Central Czech Republic (3.1 and 2.0, respectively, letter W in Fig.
692 9). Medium pollen producers comprise shrubs and herbaceous taxa, including *Erica* (1.18),
693 comparable to the value from Southern France (1.5) (letter V), *Asteraceae* sf. *Cichorioideae* (1.06)
694 and *Ranunculaceae* (1.45), the latter two aligning with values of 1.0 and 1.3, respectively, reported
695 from the White Carpathians (letter Y in Fig. 9). Low pollen producers – primarily entomophilous

696 herbs or shrubs – such as Rosaceae (0.31) and *Genista*-type/Fabaceae (0.42) correspond well with
697 previously reported values of 0.3 and 0.5 from Southeastern Romania (letter Z).

698 In contrast, other taxa did not clearly match values reported in earlier studies, either due to a
699 limited number of existing estimates or a wide variability in published data. For instance, RPP
700 values for Asteraceae sf. Asteroideae (0.31) and Brassicaceae (0.28) are among the first reported
701 or there are only a few previous estimates, making direct comparison difficult. For *Corylus* (0.94)
702 our result lies within the mid-range of previously published values, which vary considerably (Fig.
703 9). Nonetheless, these values appear consistent with biological expectations – entomophilous
704 herbs typically show lower pollen productivity than anemophilous trees – suggesting that the
705 estimates are reasonable despite limited comparative data. For some taxa, Iberian RPPs follow a
706 different trend than elsewhere in Europe, especially for *Abies* or *Betula*. When values are rescaled
707 to remove the effect of the reference taxon, *Abies* emerged as a high pollen producer in STI (2.93).
708 *Betula* (0.66) also presents lower productivity than in other European studies (Fig. 9). As
709 discussed above, this underrepresentation of the temperate forest taxa may point to the need for
710 computation of specific RPPs for the Eurosiberian biogeographical region, which is where these
711 forest taxa are mainly found in STI.

712 RPPs for *Olea* (2.60) in this study are the first estimates in Europe. Both *Olea* and evergreen
713 *Quercus* are only present in southern Europe, and therefore new RPPs in the other Mediterranean
714 peninsulas are needed in future studies to unravel the palaeoecological history of these species
715 during the Holocene. It is of critical importance to better understand the history of key pollen
716 taxa, especially when they vary their functional role in ecosystem and become narrowly linked to
717 human presence, as it happens with *Olea*, offering new insights on anthropogenic triggers in the
718 past. Indeed, *Plantago* and *Rumex*, also key taxa related to human activities, were found to present
719 lower productivities in STI than in the eight most comparable studies from elsewhere in Europe.
720 We argue two main factor explaining lower productivity of these taxa in Spain: first,
721 Mediterranean climatic conditions may constrain the growth of these herbaceous taxa, thereby
722 reducing their reproductive performance (López-Orozco et al., 2023).; and, second, traditional
723 Iberian land-use systems (e.g., extensive grazing, dehesa-like agro-silvo pastoral mosaics) tend to
724 maintain semi-open or wooded pastures rather than the continuously open, nutrient-rich
725 grasslands common in northern Europe (Connor et al., 2019).

726 *Approach limitations*

727 Reconstructing past vegetation in Iberia with REVEALS poses unique methodological constraints
728 owing to the region's pronounced topographic and environmental heterogeneity. The lack of large
729 lake basins common in northern Europe often forces reliance on smaller sedimentary basins,
730 increasing uncertainty (Sugita, 2007a). A core assumption of REVEALS is spatially consistent
731 pollen–vegetation relationships, but Iberia's uneven distribution of mixed temperate forest taxa
732 (*Betula*, *Corylus*, *Fagus*), restricted to the northern fringe, challenges this assumption. Averaging
733 RPPs across the STI may therefore underestimate productivity in optimal habitats.

734 Moreover, the surface pollen collection may have introduced spatial biases in two different ways:
735 1) overrepresentation of certain vegetation communities and 2) overrepresentation of certain taxa.
736 Both are connected to moss polsters being used as pollen traps as these are usually located in
737 humid and mountainous areas (Fig. 1), especially in the Mediterranean region, limiting the
738 representation of open vegetation landscapes from Iberia. In addition, moss polsters are
739 sometimes located under the tree canopy, especially in the Mediterranean region, perhaps
740 resulting in overrepresentation of those taxa. For instance, this could have been the case with
741 *Abies* (see Fig. S7 in the Supplement), where both species (*A. pinsapo* and *A. alba*) coexist with
742 the moss polsters in humid, cooler regions, potentially leading to higher estimates of pollen
743 productivity.

744 Vegetation datasets also introduce uncertainty. The MFE maps well the dominant tree species but
745 underrepresents taxa forming scattered stands (*J. oxycedrus*, *J. communis*), beyond the scope of
746 forestry interest. The SIVIM database contains almost 150,000 phytosociological plant
747 inventories. The frequency of the taxa is estimated on a scale of 1 to 5, which we transformed
748 into percentages of abundances (equivalence table can be found in Table S4 in the Supplement).
749 Despite the non-continuous nature of the SIVIM data, RPPs for shrub and herb taxa yielded robust
750 and ecologically meaningful results, except for *Genista*-type, whose productivity estimate was
751 lower than the standard deviation. Regarding the main source of pollen data, the EMPD2, some
752 of the samples were incomplete or misclassified (e.g., some salt lakes were not specified as such;
753 some samples had inaccurate coordinates or lacked information about the sample type or the
754 sample context).

755 Finally, the choice of a loss function could influence RPP estimates. In our work, we chose a
756 weighted sum of squared errors (WSSE) method that calculates the optimal set of taxon-specific
757 RPP values that minimises the discrepancy between observed regional vegetation composition
758 and vegetation proportions reconstructed by REVEALS. This loss function addresses two main
759 challenges in pollen-vegetation modelling: heteroskedasticity and taxon-specific biases. Pollen-
760 vegetation relationships are inherently heteroskedastic, which means that the variance of the
761 residuals scales with vegetation abundance (Sugita et al., 2010). Dominant taxa typically exhibit
762 high pollen production, leading to smaller relative errors in their vegetation estimates, while rare
763 or underrepresented taxa often show disproportionate noise due to low pollen counts and localised
764 distributions (Broström et al., 2008). In order to partially account for these uncertainties, we
765 weight errors inversely, as the WSSE function ensures that deviations for rare taxa contribute
766 meaningfully to the optimisation, preventing their signals from being overshadowed by dominant
767 taxa. By doing this, we acknowledge that residual uncertainty remains higher for the less frequent
768 taxa.

769 5. Conclusions

770 We used reverse REVEALS to produce the first pollen productivity estimates (relative to
771 Poaceae) for the Spanish Territory of Iberia. Overall, we found that conifers (*Pinus* and *Abies*),
772 both evergreen and deciduous *Quercus* and *Olea* are high pollen producers in continental Spain.
773 Temperate forest arboreal taxa were identified as medium pollen producers, while shrub and herb
774 taxa generally yielded lower RPPs, except for anemophilous taxa like Amaranthaceae.
775

776 We also performed the first extensive validation of RPPs for arboreal taxa in southern Europe,
777 using 26 present-day coretops and forest inventory data. The most frequent arboreal taxa in
778 present-day landscapes performed better with REVEALS-based estimates than with raw pollen
779 counts. Additionally, we conducted a bias-free comparison of our RPPs with other European
780 datasets, finding similar values overall, except for temperate taxa and *Abies*. Future studies should
781 examine whether more accurate estimates could be achieved by producing separate RPP datasets
782 for the Eurosiberian and Mediterranean bioclimatic regions. Region-specific RPPs, tailored to
783 bioclimatic variability, could improve the accuracy of vegetation reconstructions and disturbance
784 assessments across the Iberian Peninsula.
785

786 Finally, these findings suggest that previous reconstructions of past vegetation dynamics in the
787 Iberian Peninsula may have overestimated the presence of pines and oaks, and therefore fossil
788 records from the Southwestern Mediterranean may require reinterpretation. Future research using
789 the new relative pollen productivity estimates for Iberian taxa to generate quantitative vegetation
790 reconstructions could indicate a more mosaic-like pattern of broadleaf woodlands, conifers,
791 temperate forests and open ecosystems, aligning with most recent findings.
792

793 **Code and data availability**

794 All the code and the new RPP dataset for the Spanish Territory of Iberia are publicly available at
795 <https://doi.org/10.5281/zenodo.17927544> (Jungkeit-Milla et al., 2025). User may access to
796 download the code and to reproduce the figures in this manuscript, by using the available data in
797 Jungkeit-Milla et al. (2025). Data included are processed pollen counts and regional vegetation
798 proportions for continental Spain, present-day coretops, REVEALS estimates and rings used for
799 validation, and RPP values from different studies in Europe, in order to proceed with the
800 comparison.

801 **Supplement**

802 The supplement related to this article is available online at
803 <https://saco.csic.es/s/9NJE9GwqLdzAJkQ>

804 **Author contributions following CRedit**

805 Conceptualisation: GGR, PGS. Methodology: VA, KJM, GGR, PGS. Software: KJM, VA.
806 Validation: KJM, MM. Formal analysis: VA, KJM. Investigation: KJM, GGR, PGS. Data
807 curation: KJM, VA. Resources: GGR, PGS, XF, MF, FM, FFM, HSO. Writing - Original Draft:
808 KJM, VA, GGR, PGS, HR, EGP. Writing - Review & Editing: MS, JA, ML, MF, FFM, MM,
809 PGS, GGR. Visualisation: KJM, VA, MS. Funding acquisition: GGR, PGS, KJM.

810 **Acknowledgements**

811 Numerous people helped guide this work over the last years. The authors would like to
812 acknowledge Scientific and Technique Analysis Services in Pyrenean Institute of Ecology-CSIC
813 in Zaragoza (Spain) for their technical and analytical support, especially Elena Royo and Aida
814 Adsuar for the laboratory work. We also thank Pedro Sánchez Navarrete and Antonio Vallejo for
815 their help in the field campaigns. We are grateful to Jane Bunting for initial support on the use
816 of ERV models. We thank Alastair Wills for his suggestions regarding regionalisation, as well as
817 for the discussions that helped us to improve this manuscript. We are grateful to the European
818 Pollen Database and Neotoma communities for their altruistic work that fosters free, open palaeo-
819 science. We acknowledge that AI has been used to assist in the revision of the final code.

820 **Financial support**

821 CORREDORAS (ref: PID2022-141558NB-I00), PYCACHU (ref: PID2019-106050RB-I00),
822 DINAMO 3 (ref: CGL2015-69160-R, DINAMO 2 (ref: CGL2012-33063), DINAMO 1 (ref:
823 CGL2009-07992), and FPU Research Grants (FPU22/01191).

824 **References**

825 Abraham, V. and Kozáková, R.: Relative pollen productivity estimates in the modern agricultural
826 landscape of Central Bohemia (Czech Republic), *Rev. Palaeobot. Palynol.*, 179, 1–12,
827 <https://doi.org/10.1016/j.revpalbo.2012.04.004>, 2012.

828 Abrantes, F., Voelker, A. (Helga L., Sierro, F. J., Naughton, F., Rodrigues, T., Cacho, I.,
829 Ariztegui, D., Brayshaw, D., Sicre, M.-A., and Batista, L.: Paleoclimate Variability in the
830 Mediterranean Region, in: *The Climate of the Mediterranean Region*, Elsevier, 1–86,
831 <https://doi.org/10.1016/B978-0-12-416042-2.00001-X>, 2012.

832 Andersen, M.: Mechanistic Models for the Seed Shadows of Wind-Dispersed Plants, *Am. Nat.*,
833 137, 476–497, <https://doi.org/10.1086/285178>, 1991.

834 Andersen, S. Th.: The Relative Pollen Productivity and Pollen Representation of North European
835 Trees, and Correction Factors for Tree Pollen Spectra. Determined by Surface Pollen Analyses

836 from *Forests, Dan. Geol. Unders. II* Række, 96, 1–99, <https://doi.org/10.34194/raekke2.v96.6887>,
837 1970.

838 Aranbarri, J., González-Sampériz, P., Valero-Garcés, B., Moreno, A., Gil-Romera, G., Sevilla-
839 Callejo, M., García-Prieto, E., Di Rita, F., Mata, M. P., Morellón, M., Magri, D., Rodríguez-
840 Lázaro, J., and Carrión, J. S.: Rapid climatic changes and resilient vegetation during the
841 Lateglacial and Holocene in a continental region of south-western Europe, *Glob. Planet. Change*,
842 114, 50–65, <https://doi.org/10.1016/j.gloplacha.2014.01.003>, 2014.

843 Aranbarri, J., Alcolea, M., Badal, E., Vila, S., Allué, E., Iriarte-Chiapusso, M. J., Sebastián, M.,
844 Magri, D., and González-Sampériz, P.: Holocene history of Aleppo pine (*Pinus halepensis* Mill.)
845 woodlands in the Ebro Basin (NE Spain): Climate-biased or human-induced?, *Rev. Palaeobot.*
846 *Palynol.*, 279, 104240, <https://doi.org/10.1016/j.revpalbo.2020.104240>, 2020.

847 Baker, A. G., Zimny, M., Keczyński, A., Bhagwat, S. A., Willis, K. J., and Latałowa, M.: Pollen
848 productivity estimates from old-growth forest strongly differ from those obtained in cultural
849 landscapes: Evidence from the Białowieża National Park, Poland, *The Holocene*, 26, 80–92,
850 <https://doi.org/10.1177/0959683615596822>, 2016.

851 Broström, A., Sugita, S., and Gaillard, M.-J.: Pollen productivity estimates for the reconstruction
852 of past vegetation cover in the cultural landscape of southern Sweden, *The Holocene*, 14, 368–
853 381, <https://doi.org/10.1191/0959683604hl713rp>, 2004.

854 Broström, A., Sugita, S., Gaillard, M.-J., and Pilesjö, P.: Estimating the spatial scale of pollen
855 dispersal in the cultural landscape of southern Sweden, *The Holocene*, 15, 252–262,
856 <https://doi.org/10.1191/0959683605hl790rp>, 2005.

857 Broström, A., Nielsen, A. B., Gaillard, M.-J., Hjelle, K., Mazier, F., Binney, H., Bunting, J., Fyfe,
858 R., Meltssov, V., Poska, A., Räsänen, S., Soepboer, W., von Stedingk, H., Suutari, H., and Sugita,
859 S.: Pollen productivity estimates of key European plant taxa for quantitative reconstruction of
860 past vegetation: a review, *Veg. Hist. Archaeobotany*, 17, 461–478,
861 <https://doi.org/10.1007/s00334-008-0148-8>, 2008.

862 Bunting, M. J., Armitage, R., Binney, H. A., and Waller, M.: Estimates of ‘relative pollen
863 productivity’ and ‘relevant source area of pollen’ for major tree taxa in two Norfolk (UK)
864 woodlands, *The Holocene*, 15, 459–465, <https://doi.org/10.1191/0959683605hl821rr>, 2005.

865 Calcote, R.: Pollen Source Area and Pollen Productivity: Evidence from Forest Hollows, *J. Ecol.*,
866 83, 591, <https://doi.org/10.2307/2261627>, 1995.

867 Cañellas-Boltà, N., Rull, V., Vigo, J., and Mercadé, A.: Modern pollen—vegetation relationships
868 along an altitudinal transect in the central Pyrenees (southwestern Europe), *The Holocene*, 19,
869 1185–1200, <https://doi.org/10.1177/0959683609345082>, 2009.

870 Carrión, J., Lopez-Saez, J., Casas-Gallego, M., Gonzalez-Samperiz, P., Badal, E., Perez-Diaz, S.,
871 Carrion-Marco, Y., Jimenez-Moreno, G., Lopez-Merino, L., Burjachs, F., Abel-Schaad, D.,
872 Fernandez, S., Morales-Molino, C., Alba Sanchez, F., Peña-Chocarro, L., Barron, E., Postigo-
873 Mijarra, J., Gil-Garcia, M., Rubiales, J., Vidal-Matutano, P., Arambarri, J., Ramos-Roman, M.,
874 Camuera, J., Magri, D., Revelles, J., Altolaguirre, Y., Ruiz-Zapata, B., Luelmo, R., Uzquiano, P.,
875 Allué, E., Anderson, S., Dupre, M., Gil-Romera, G., Pique, R., Garcia-Anton, M., Amoros, G.,
876 Yll, R., Perez-Jorda, G., Scott, L., Figueiral, I., Rodriguez-Ariza, M., Morla-Jauristi, C., Garcia-
877 Amorena, I., Montoya, E., Val Peon, C., Ejarque, A., Riera, S., Peñalba, C., Fierro, E., Exposito,
878 I., Perez-Obiol, R., Vieira, M., Gomez-Manzaneque, F., Maldonado, J., Leunda, M., Franco, F.,
879 Albert, R., Diez, M., Marin-Arroyo, A., Manzano, S., Dirita, F., Andrade, A., Parra, I., Zapata,
880 L., Perez, A., Grau, E., Alcolea, M., Mesa-Fernandez, J., Miras, Y., Ruiz-Alonso, M., Genova,

881 M., Garcia-Alvarez, S., Moreno, E., Olmedo Cobo, J., Gomez Zotano, J., Pardo Martinez, R.,
882 Mas, B., Monteiro, P., Antolin, F., Obea, L., Martin-Seijo, M., Alonso, N., Amoros, A.,
883 Fernandez-Diaz, M., Reyes, P., Sanchez-Giner, V., Gomez-Rodriguez, M., Rull, V., Vegas-
884 Villarrubia, T., Lopez-Bulto, O., Bianco, S., Trapote, M., Picornell-Gelabert, L., Sureda, P.,
885 Brisset, E., Servera Vives, G., Girona, A., Celant, A., Munuera, M., et al.: Paleoflora y
886 Paleovegetación Ibérica III: Holoceno, edited by: Séneca, M. de C. e I. y F., 1095 pp., 2022.

887 Carrión, J. S., Yll, E. I., Willis, K. J., and Sánchez, P.: Holocene forest history of the eastern
888 plateaux in the Segura Mountains (Murcia, southeastern Spain), *Rev. Palaeobot. Palynol.*, 132,
889 219–236, <https://doi.org/10.1016/j.revpalbo.2004.07.002>, 2004.

890 Carrión, J. S., Fernández, S., González-Sampériz, P., Gil-Romera, G., Badal, E., Carrión-Marco,
891 Y., López-Merino, L., López-Sáez, J. A., Fierro, E., and Burjachs, F.: Expected trends and
892 surprises in the Lateglacial and Holocene vegetation history of the Iberian Peninsula and Balearic
893 Islands, *Rev. Palaeobot. Palynol.*, 162, 458–475, <https://doi.org/10.1016/j.revpalbo.2009.12.007>,
894 2010a.

895 Carrión, Y., Ntinou, M., and Badal, E.: *Olea europaea* L. in the North Mediterranean Basin during
896 the Pleniglacial and the Early–Middle Holocene, *Quat. Sci. Rev.*, 29, 952–968,
897 <https://doi.org/10.1016/j.quascirev.2009.12.015>, 2010b.

898 Carroll, R. J. and Ruppert, D.: Transformation and weighting in regression, Chapman and Hall,
899 New York, 1988.

900 Castroviejo, S.: Flora iberica 1-8, 10-15, 17-18, 21, 2012.

901 Chaput, M. A. and Gajewski, K.: Relative pollen productivity estimates and changes in Holocene
902 vegetation cover in the deciduous forest of southeastern Quebec, Canada, *Botany*, 96, 299–317,
903 <https://doi.org/10.1139/cjb-2017-0193>, 2018.

904 Chazarra, A., Flórez-García, E., Peraza-Sánchez, B., Tohá-Rebull, T., Lorenzo-Mariño, B.,
905 Criado-Pinto, E., Moreno-García, J. V., Romero-Fresneda, R., and Botez-Fullat, R.: Mapas
906 climáticos de España (1981-2010) y ETo (1996-2016), Agencia Estatal de Meteorología,
907 <https://doi.org/10.31978/014-18-004-2>, 2018.

908 Cheddadi, R., Lamb, H. F., Guiot, J., and Van Der Kaars, S.: Holocene climatic change in
909 Morocco: a quantitative reconstruction from pollen data, *Clim. Dyn.*, 14, 883–890,
910 <https://doi.org/10.1007/s003820050262>, 1998.

911 Commerford, J. L., McLauchlan, K. K., and Sugita, S.: Calibrating vegetation cover and grassland
912 pollen assemblages in the Flint Hills of Kansas, USA, *Am. J. Plant Sci.*, 4, 1–10,
913 <https://doi.org/10.4236/ajps.2013.47A1001>, 2013.

914 Connor, S. E., Vannière, B., Colombaroli, D., Anderson, R. S., Carrión, J. S., Ejarque, A., Gil
915 Romera, G., González-Sampériz, P., Hoefer, D., Morales-Molino, C., Revelles, J., Schneider, H.,
916 Van Der Knaap, W. O., Van Leeuwen, J. F., and Woodbridge, J.: Humans take control of fire-
917 driven diversity changes in Mediterranean Iberia's vegetation during the mid–late Holocene, *The
918 Holocene*, 29, 886–901, <https://doi.org/10.1177/0959683619826652>, 2019.

919 Costa, M., Morla, C., and Sainz-Ollero, H.: Los bosques ibéricos. Una interpretación
920 geobotánica., Planeta, 598 pp., 1998.

921 Cowling, R. M., Rundel, P. W., Lamont, B. B., Kalin Arroyo, M., and Arianoutsou, M.: Plant
922 diversity in mediterranean-climate regions, *Trends Ecol. Evol.*, 11, 362–366,
923 [https://doi.org/10.1016/0169-5347\(96\)10044-6](https://doi.org/10.1016/0169-5347(96)10044-6), 1996.

924 Davis, B. A. S., Chevalier, M., Sommer, P., Carter, V. A., Finsinger, W., Mauri, A., Phelps, L.
925 N., Zanon, M., Abegglen, R., Åkesson, C. M., Alba-Sánchez, F., Anderson, R. S., Antipina, T.
926 G., Atanassova, J. R., Beer, R., Belyanina, N. I., Blyakharchuk, T. A., Borisova, O. K., Bozilova,
927 E., Bukreeva, G., Bunting, M. J., Clò, E., Colombaroli, D., Combourieu-Nebout, N., Desprat, S.,
928 Di Rita, F., Djamali, M., Edwards, K. J., Fall, P. L., Feurdean, A., Fletcher, W., Florenzano, A.,
929 Furlanetto, G., Gaceur, E., Galimov, A. T., Gałka, M., Garcia-Moreiras, I., Giesecke, T.,
930 Grindean, R., Guido, M. A., Gvozdeva, I. G., Herzschuh, U., Hjelle, K. L., Ivanov, S., Jahns, S.,
931 Jankovska, V., Jiménez-Moreno, G., Karpińska-Kołaczek, M., Kitaba, I., Kołaczek, P., Lapteva,
932 E. G., Latałowa, M., Lebreton, V., Leroy, S., Leydet, M., Lopatina, D. A., López-Sáez, J. A.,
933 Lotter, A. F., Magri, D., Marinova, E., Matthias, I., Mavridou, A., Mercuri, A. M., Mesa-
934 Fernández, J. M., Mikishin, Y. A., Milecka, K., Montanari, C., Morales-Molino, C., Mrotzek, A.,
935 Muñoz Sobrino, C., Naidina, O. D., Nakagawa, T., Nielsen, A. B., Novenko, E. Y., Panajotidis,
936 S., Panova, N. K., Papadopoulou, M., Pardoe, H. S., Pędziszewska, A., Petrenko, T. I., Ramos-
937 Román, M. J., Ravazzi, C., Rösch, M., Ryabogina, N., Sabariego Ruiz, S., Salonen, J. S., Sapelko,
938 T. V., Schofield, J. E., Seppä, H., Shumilovskikh, L., Stivrins, N., Stojakowits, P., Svobodova
939 Svitavska, H., Święta-Musznicka, J., Tantau, I., Tinner, W., Tobolski, K., Tonkov, S., Tsakiridou,
940 M., et al.: The Eurasian Modern Pollen Database (EMPD), version 2, *Earth Syst. Sci. Data*, 12,
941 2423–2445, <https://doi.org/10.5194/essd-12-2423-2020>, 2020.

942 Davis, M. B.: On the theory of pollen analysis, *Am. J. Sci.*, 261, 897–912, 1963.

943 Dawson, A., Paciorek, C. J., McLachlan, J. S., Goring, S., Williams, J. W., and Jackson, S. T.:
944 Quantifying pollen-vegetation relationships to reconstruct ancient forests using 19th-century
945 forest composition and pollen data, *Quat. Sci. Rev.*, 137, 156–175,
946 <https://doi.org/10.1016/j.quascirev.2016.01.012>, 2016.

947 Duffin, K. I. and Bunting, M. J.: Relative pollen productivity and fall speed estimates for southern
948 African savanna taxa, *Veg. Hist. Archaeobotany*, 17, 507–525, <https://doi.org/10.1007/s00334-007-0101-2>, 2008.

949 Ellis, E. C.: Land Use and Ecological Change: A 12,000-Year History, *Annu. Rev. Environ.*
950 *Resour.*, 46, 1–33, <https://doi.org/10.1146/annurev-environ-012220-010822>, 2021.

952 Ergin, E., Marquer, L., Mazier, F., Bisson, U., and Dalfes, H. N.: Relative Pollen Productivity
953 Estimates for Mediterranean Plant Taxa: A New Study Region in Turkey, *Land*, 13, 591,
954 <https://doi.org/10.3390/land13050591>, 2024.

955 European Environment Agency: CORINE Land Cover 2018 (vector), Europe, 6-yearly - version
956 2020_20u1, May 2020 (20.01), <https://doi.org/10.2909/71C95A07-E296-44FC-B22B-415F42ACFDF0>, 2019.

958 Ezquerra, F. J., Cañas, I., Oria-de-Rueda, J. A., and Rubiales, J. M.: Late-Holocene fossil
959 evidence and the interpretation of the vegetation in NW Iberia: management issues in the light of
960 palaeoecological findings, *Veg. Hist. Archaeobotany*, 28, 35–50, <https://doi.org/10.1007/s00334-018-0684-9>, 2019.

962 Fang, Y., Ma, C., and Bunting, M. J.: Novel methods of estimating relative pollen productivity:
963 A key parameter for reconstruction of past land cover from pollen records, *Prog. Phys. Geogr.*
964 *Earth Environ.*, 43, 731–753, <https://doi.org/10.1177/0309133319861808>, 2019.

965 Fernández, S., Fuentes, N., Carrión, J. S., González-Sampériz, P., Montoya, E., Gil, G., Vega-
966 Toscano, G., and Riquelme, J. A.: The Holocene and Upper Pleistocene pollen sequence of
967 Carihuella Cave, southern Spain, *Geobios*, 40, 75–90,
968 <https://doi.org/10.1016/j.geobios.2006.01.004>, 2007.

969 Fernández-Rodríguez, S., Skjøth, C. A., Tormo-Molina, R., Brandao, R., Caeiro, E., Silva-
970 Palacios, I., Gonzalo-Garijo, Á., and Smith, M.: Identification of potential sources of airborne
971 Olea pollen in the Southwest Iberian Peninsula, *Int. J. Biometeorol.*, 58, 337–348,
972 <https://doi.org/10.1007/s00484-012-0629-4>, 2014.

973 Font, X., Balcells, L., and Mora, B.: The Plot-Based Databases of the Iberian Vegetation, in: The
974 Vegetation of the Iberian Peninsula, vol. 13, edited by: Loidi, J., Springer International
975 Publishing, Cham, 565–579, https://doi.org/10.1007/978-3-319-54867-8_13, 2017.

976 Fyfe, R. M., Woodbridge, J., and Roberts, N.: From forest to farmland: pollen-inferred land cover
977 change across Europe using the pseudobiomization approach, *Glob. Change Biol.*, 21, 1197–
978 1212, <https://doi.org/10.1111/gcb.12776>, 2015.

979 Garreta, V., Guiot, J., Mortier, F., Chadœuf, J., and Hély, C.: Pollen-based climate reconstruction:
980 Calibration of the vegetation–pollen processes, *Ecol. Model.*, 235–236, 81–94,
981 <https://doi.org/10.1016/j.ecolmodel.2012.03.031>, 2012.

982 Gavilán, R. G., Vilches, B., Gutiérrez-Girón, A., Blanquer, J. M., and Escudero, A.:
983 Sclerophyllous Versus Deciduous Forests in the Iberian Peninsula: A Standard Case of
984 Mediterranean Climatic Vegetation Distribution, in: Geographical Changes in Vegetation and
985 Plant Functional Types, edited by: Greller, A. M., Fujiwara, K., and Pedrotti, F., Springer
986 International Publishing, Cham, 101–116, https://doi.org/10.1007/978-3-319-68738-4_5, 2018.

987 Gil-Romera, G., González-Sampériz, P., Lasheras-Álvarez, L., Sevilla-Callejo, M., Moreno, A.,
988 Valero-Garcés, B., López-Merino, L., Carrión, J. S., Pérez Sanz, A., Aranbarri, J., and García-
989 Prieto Fronce, E.: Biomass-modulated fire dynamics during the Last Glacial–Interglacial
990 Transition at the Central Pyrenees (Spain), *Palaeogeogr. Palaeoclimatol. Palaeoecol.*, 402, 113–
991 124, <https://doi.org/10.1016/j.palaeo.2014.03.015>, 2014.

992 Githumbi, E., Fyfe, R., Gaillard, M.-J., Trondman, A.-K., Mazier, F., Nielsen, A.-B., Poska, A.,
993 Sugita, S., Woodbridge, J., Azuara, J., Feurdean, A., Grindean, R., Lebreton, V., Marquer, L.,
994 Nebout-Combouieu, N., Stančikaitė, M., Tančāu, I., Tonkov, S., Shumilovskikh, L., and
995 LandClimII data contributors: European pollen-based REVEALS land-cover reconstructions for
996 the Holocene: methodology, mapping and potentials, *Earth Syst. Sci. Data*, 14, 1581–1619,
997 <https://doi.org/10.5194/essd-14-1581-2022>, 2022.

998 Gomes, S. D., Fletcher, W. J., Rodrigues, T., Stone, A., Abrantes, F., and Naughton, F.: Time-
999 transgressive Holocene maximum of temperate and Mediterranean forest development across the
1000 Iberian Peninsula reflects orbital forcing, *Palaeogeogr. Palaeoclimatol. Palaeoecol.*, 550, 109739,
1001 <https://doi.org/10.1016/j.palaeo.2020.109739>, 2020.

1002 González-Sampériz, P., Valero-Garcés, B. L., Moreno, A., Jalut, G., García-Ruiz, J. M., Martí-
1003 Bono, C., Delgado-Huertas, A., Navas, A., Otto, T., and Dedoubat, J. J.: Climate variability in the
1004 Spanish Pyrenees during the last 30,000 yr revealed by the El Portalet sequence, *Quat. Res.*, 66,
1005 38–52, <https://doi.org/10.1016/j.yqres.2006.02.004>, 2006.

1006 González-Sampériz, P., Leroy, S. A. G., Carrión, J. S., Fernández, S., García-Antón, M., Gil-
1007 García, M. J., Uzquiano, P., Valero-Garcés, B., and Figueiral, I.: Steppes, savannahs, forests and
1008 phytodiversity reservoirs during the Pleistocene in the Iberian Peninsula, *Rev. Palaeobot. Palynol.*, 162, 427–457,
1009 <https://doi.org/10.1016/j.revpalbo.2010.03.009>, 2010.

1010 González-Sampériz, P., Gil-Romera, G., García-Prieto, E., Aranbarri, J., Moreno, A., Morellón,
1011 M., Sevilla-Callejo, M., Leunda, M., Santos, L., Franco-Múgica, F., Andrade, A., Carrión, J. S.,
1012 and Valero-Garcés, B. L.: Strong continentality and effective moisture drove unforeseen
1013 vegetation dynamics since the last interglacial at inland Mediterranean areas: The Villarquemado

1014 sequence in NE Iberia, *Quat. Sci. Rev.*, 242, 106425,
1015 <https://doi.org/10.1016/j.quascirev.2020.106425>, 2020.

1016 Gregory, P. H.: The microbiology of the atmosphere, 2nd edition., Leonard Hill, Aylesbury,
1017 London, 1961.

1018 Grindean, R., Nielsen, A. B., Tanțău, I., and Feurdean, A.: Relative pollen productivity estimates
1019 in the forest steppe landscape of southeastern Romania, *Rev. Palaeobot. Palynol.*, 264, 54–63,
1020 <https://doi.org/10.1016/j.revpalbo.2019.02.007>, 2019.

1021 Han, Y., Liu, H., Hao, Q., Liu, X., Guo, W., and Shangguan, H.: More reliable pollen productivity
1022 estimates and relative source area of pollen in a forest-steppe ecotone with improved vegetation
1023 survey, *The Holocene*, 27, 1567–1577, <https://doi.org/10.1177/0959683617702234>, 2017.

1024 He, F., Li, Y., Wu, J., and Xu, Y.: A comparison of relative pollen productivity from forest steppe,
1025 typical steppe and desert steppe in Inner Mongolia, *Chin. Sci. Bull.*, 61, 3388–3400,
1026 <https://doi.org/10.1360/N972016-00482>, 2016.

1027 Hellman, S., Gaillard, M.-J., Broström, A., and Sugita, S.: The REVEALS model, a new tool to
1028 estimate past regional plant abundance from pollen data in large lakes: validation in southern
1029 Sweden, *J. Quat. Sci.*, 23, 21–42, <https://doi.org/10.1002/jqs.1126>, 2008.

1030 Hjelle, K. L.: Herb pollen representation in surface moss samples from mown meadows and
1031 pastures in western Norway, *Veg. Hist. Archaeobotany*, 7, 79–96,
1032 <https://doi.org/10.1007/BF01373926>, 1998.

1033 Huntley, B.: European vegetation history: Palaeovegetation maps from pollen data - 13 000 yr BP
1034 to present, *J. Quat. Sci.*, 5, 103–122, <https://doi.org/10.1002/jqs.3390050203>, 1990.

1035 IPCC: Climate Change 2022 – Impacts, Adaptation and Vulnerability: Working Group II
1036 Contribution to the Sixth Assessment Report of the Intergovernmental Panel on Climate Change,
1037 1st ed., Cambridge University Press, <https://doi.org/10.1017/9781009325844>, 2023.

1038 Jackson, S. T. and Lyford, M. E.: Pollen dispersal models in Quaternary plant ecology:
1039 Assumptions, parameters, and prescriptions, *Bot. Rev.*, 65, 39–75,
1040 <https://doi.org/10.1007/BF02856557>, 1999.

1041 Jiang, F., Xu, Q., Zhang, S., Li, F., Zhang, K., Wang, M., Shen, W., Sun, Y., and Zhou, Z.:
1042 Relative pollen productivities of the major plant taxa of subtropical evergreen–deciduous mixed
1043 woodland in China, *J. Quat. Sci.*, 35, 526–538, <https://doi.org/10.1002/jqs.3197>, 2020.

1044 Jungkeit-Milla, K., Abraham, V., González-Sampériz, P., and Gil-Romera, G.: Novel relative
1045 pollen productivity estimates for the Western Mediterranean - Code and dataset,
1046 <https://doi.org/10.5281/ZENODO.17927544>, 2025.

1047 Katul, G. G., Porporato, A., Nathan, R., Siqueira, M., Soons, M. B., Poggi, D., Horn, H. S., and
1048 Levin, S. A.: Mechanistic Analytical Models for Long-Distance Seed Dispersal by Wind, *Am. Nat.*, 166, 368–381, <https://doi.org/10.1086/432589>, 2005.

1050 Knight, C. A., Battles, J. J., Bunting, M. J., Champagne, M., Wanket, J. A., and Wahl, D. B.:
1051 Methods for robust estimates of tree biomass from pollen accumulation rates: Quantifying
1052 paleoecological reconstruction uncertainty, *Front. Ecol. Evol.*, 10, 956143,
1053 <https://doi.org/10.3389/fevo.2022.956143>, 2022.

1054 Kuneš, P., Abraham, V., Werchan, B., Plesková, Z., Fajmon, K., Jamrichová, E., and Roleček, J.:
1055 Relative pollen productivity estimates for vegetation reconstruction in central-eastern Europe

1056 inferred at local and regional scales, *The Holocene*, 29, 1708–1719,
1057 <https://doi.org/10.1177/0959683619862026>, 2019.

1058 Kuparinen, A.: Mechanistic models for wind dispersal, *Trends Plant Sci.*, 11, 296–301,
1059 <https://doi.org/10.1016/j.tplants.2006.04.006>, 2006.

1060 Kuparinen, A., Markkanen, T., Riikonen, H., and Vesala, T.: Modeling air-mediated dispersal of
1061 spores, pollen and seeds in forested areas, *Ecol. Model.*, 208, 177–188,
1062 <https://doi.org/10.1016/j.ecolmodel.2007.05.023>, 2007.

1063 Langgut, D., Cheddadi, R., Carrión, J. S., Cavanagh, M., Colombaroli, D., Eastwood, W. J.,
1064 Greenberg, R., Litt, T., Mercuri, A. M., Miebach, A., Roberts, C. N., Woldring, H., and
1065 Woodbridge, J.: The origin and spread of olive cultivation in the Mediterranean Basin: The fossil
1066 pollen evidence, *The Holocene*, 29, 902–922, <https://doi.org/10.1177/0959683619826654>, 2019.

1067 Leunda, M., González-Sampériz, P., Gil-Romera, G., Aranbarri, J., Moreno, A., Oliva-Urcia, B.,
1068 Sevilla-Callejo, M., and Valero-Garcés, B.: The Late-Glacial and Holocene Marboré Lake
1069 sequence (2612 m a.s.l., Central Pyrenees, Spain): Testing high altitude sites sensitivity to
1070 millennial scale vegetation and climate variability, *Glob. Planet. Change*, 157, 214–231,
1071 <https://doi.org/10.1016/j.gloplacha.2017.08.008>, 2017.

1072 Leunda, M., Gil-Romera, G., Daniau, A.-L., Benito, B. M., and González-Sampériz, P.: Holocene
1073 fire and vegetation dynamics in the Central Pyrenees (Spain), *CATENA*, 188, 104411,
1074 <https://doi.org/10.1016/j.catena.2019.104411>, 2020.

1075 Li, F., Gaillard, M.-J., Xie, S., Huang, K., Cui, Q., Fyfe, R., Marquer, L., and Sugita, S.:
1076 Evaluation of relative pollen productivities in temperate China for reliable pollen-based
1077 quantitative reconstructions of Holocene plant cover, *Front. Plant Sci.*, 14, 1240485,
1078 <https://doi.org/10.3389/fpls.2023.1240485>, 2023.

1079 Li, Y., Bunting, M. J., Xu, Q., Jiang, S., Ding, W., and Hun, L.: Pollen-vegetation-climate
1080 relationships in some desert and desert-steppe communities in northern China, *The Holocene*, 21,
1081 997–1010, <https://doi.org/10.1177/0959683611400202>, 2011.

1082 Liu, M., Shen, Y., González-Sampériz, P., Gil-Romera, G., Ter Braak, C. J. F., Prentice, I. C.,
1083 and Harrison, S. P.: Holocene climates of the Iberian Peninsula: pollen-based reconstructions of
1084 changes in the west–east gradient of temperature and moisture, *Clim. Past*, 19, 803–834,
1085 <https://doi.org/10.5194/cp-19-803-2023>, 2023.

1086 Liu, Y., Ogle, K., Lichstein, J. W., and Jackson, S. T.: Estimation of pollen productivity and
1087 dispersal: How pollen assemblages in small lakes represent vegetation, *Ecol. Monogr.*,
1088 <https://doi.org/10.1002/ecm.1513>, 2022.

1089 López-Orozco, R., García-Mozo, H., Oteros, J., and Galán, C.: Long-term trends and influence
1090 of climate and land-use changes on pollen profiles of a Mediterranean oak forest, *Sci. Total
1091 Environ.*, 897, 165400, <https://doi.org/10.1016/j.scitotenv.2023.165400>, 2023.

1092 Maestre, F. T., Benito, B. M., Berdugo, M., Concostrina-Zubiri, L., Delgado-Baquerizo, M.,
1093 Eldridge, D. J., Guirado, E., Gross, N., Kéfi, S., Le Bagousse-Pinguet, Y., Ochoa-Hueso, R., and
1094 Soliveres, S.: Biogeography of global drylands, *New Phytol.*, 231, 540–558,
1095 <https://doi.org/10.1111/nph.17395>, 2021.

1096 Magri, D., Di Rita, F., Aranbarri, J., Fletcher, W., and González-Sampériz, P.: Quaternary
1097 disappearance of tree taxa from Southern Europe: Timing and trends, *Quat. Sci. Rev.*, 163, 23–
1098 55, <https://doi.org/10.1016/j.quascirev.2017.02.014>, 2017.

1099 Mariani, M., Connor, S. E., Theuerkauf, M., Kuneš, P., and Fletcher, M.-S.: Testing quantitative
1100 pollen dispersal models in animal-pollinated vegetation mosaics: An example from temperate
1101 Tasmania, Australia, *Quat. Sci. Rev.*, 154, 214–225,
1102 <https://doi.org/10.1016/j.quascirev.2016.10.020>, 2016.

1103 Mariani, M., Connor, S. E., Fletcher, M., Theuerkauf, M., Kuneš, P., Jacobsen, G., Saunders, K.
1104 M., and Zawadzki, A.: How old is the Tasmanian cultural landscape? A test of landscape openness
1105 using quantitative land-cover reconstructions, *J. Biogeogr.*, 44, 2410–2420,
1106 <https://doi.org/10.1111/jbi.13040>, 2017.

1107 Mariani, M., Connor, S. E., Theuerkauf, M., Herbert, A., Kuneš, P., Bowman, D., Fletcher, M.,
1108 Head, L., Kershaw, A. P., Haberle, S. G., Stevenson, J., Adeleye, M., Cadd, H., Hopf, F., and
1109 Briles, C.: Disruption of cultural burning promotes shrub encroachment and unprecedented
1110 wildfires, *Front. Ecol. Environ.*, 20, 292–300, <https://doi.org/10.1002/fee.2395>, 2022.

1111 Marquer, L., Mazier, F., Sugita, S., Galop, D., Houet, T., Faure, E., Gaillard, M.-J., Haunold, S.,
1112 de Munnik, N., Simonneau, A., De Vleeschouwer, F., and Le Roux, G.: Pollen-based
1113 reconstruction of Holocene land-cover in mountain regions: Evaluation of the Landscape
1114 Reconstruction Algorithm in the Vicdessos valley, northern Pyrenees, France, *Quat. Sci. Rev.*,
1115 228, 106049, <https://doi.org/10.1016/j.quascirev.2019.106049>, 2020.

1116 Martín-Puertas, C., Valero-Garcés, B. L., Pilar Mata, M., González-Sampériz, P., Bao, R.,
1117 Moreno, A., and Stefanova, V.: Arid and humid phases in southern Spain during the last 4000
1118 years: the Zoñar Lake record, Córdoba, *The Holocene*, 18, 907–921,
1119 <https://doi.org/10.1177/0959683608093533>, 2008.

1120 Mazier, F., Broström, A., Gaillard, M.-J., Sugita, S., Vittoz, P., and Buttler, A.: Pollen
1121 productivity estimates and relevant source area of pollen for selected plant taxa in a pasture
1122 woodland landscape of the Jura Mountains (Switzerland), *Veg. Hist. Archaeobotany*, 17, 479–
1123 495, <https://doi.org/10.1007/s00334-008-0143-0>, 2008.

1124 Médail, F. and Quézel, P.: Biodiversity Hotspots in the Mediterranean Basin: Setting Global
1125 Conservation Priorities, *Conserv. Biol.*, 13, 1510–1513, <https://doi.org/10.1046/j.1523-1739.1999.98467.x>, 1999.

1127 Microsoft and Weston, S.: `foreach`: Provides Foreach Looping Construct,
1128 <https://doi.org/10.32614/CRAN.package.foreach>, 2009.

1129 Microsoft and Weston, S.: `doParallel`: Foreach Parallel Adaptor for the “parallel” Package,
1130 <https://doi.org/10.32614/CRAN.package.doParallel>, 2011.

1131 MITECO: Mapa Forestal de España (MFE) de máxima actualidad, 2024.

1132 Morrison, K. D., Hammer, E., Boles, O., Madella, M., Whitehouse, N., Gaillard, M.-J., Bates, J.,
1133 Vander Linden, M., Merlo, S., Yao, A., Popova, L., Hill, A. C., Antolin, F., Bauer, A., Biagetti,
1134 S., Bishop, R. R., Buckland, P., Cruz, P., Dreslerová, D., Dusseldorp, G., Ellis, E., Filipovic, D.,
1135 Foster, T., Hannaford, M. J., Harrison, S. P., Hazarika, M., Herold, H., Hilpert, J., Kaplan, J. O.,
1136 Kay, A., Klein Goldewijk, K., Kolář, J., Kyazike, E., Laabs, J., Lancelotti, C., Lane, P., Lawrence,
1137 D., Lewis, K., Lombardo, U., Lucarini, G., Arroyo-Kalin, M., Marchant, R., Mayle, F.,
1138 McClatchie, M., McLeester, M., Mooney, S., Moskal-del Hoyo, M., Navarrete, V., Ndiema, E.,
1139 Góes Neves, E., Nowak, M., Out, W. A., Petrie, C., Phelps, L. N., Pinke, Z., Rostain, S., Russell,
1140 T., Sluyter, A., Styring, A. K., Tamanaha, E., Thomas, E., Veerasamy, S., Welton, L., and Zanon,
1141 M.: Mapping past human land use using archaeological data: A new classification for global land
1142 use synthesis and data harmonization, *PLOS ONE*, 16, e0246662,
1143 <https://doi.org/10.1371/journal.pone.0246662>, 2021.

1144 Múgica, F. F., Antón, M. G., Ruiz, J. M., Juaristi, C. M., and Ollerol, H. S.: The Holocene history
1145 of *Pinnus* forests in the Spanish Northern Meseta, *The Holocene*, 11, 343–358,
1146 <https://doi.org/10.1191/095968301669474913>, 2001.

1147 Mullen, K., Ardia, D., Gil, D., Windover, D., and Cline, J.: DEoptim : An R Package for Global
1148 Optimization by Differential Evolution, *J. Stat. Softw.*, 40, <https://doi.org/10.18637/jss.v040.i06>,
1149 2011.

1150 Mutke, S., Gordo, J., Chambel, M. R., Prada, M. A., Álvarez, D., Iglesias, S., and Gil, L.:
1151 Phenotypic plasticity is stronger than adaptative differentiation among Mediterranean stone pine
1152 provenances, *For. Syst.*, 19, 354–366, <https://doi.org/10.5424/fs/2010193-9097>, 2010.

1153 Nielsen, A. B.: Modelling pollen sedimentation in Danish lakes at *c.* AD 1800: an attempt to
1154 validate the POLLSCAPE model, *J. Biogeogr.*, 31, 1693–1709, <https://doi.org/10.1111/j.1365-2699.2004.01080.x>, 2004.

1156 Niemeyer, B., Klemm, J., Pestryakova, L. A., and Herzschuh, U.: Relative pollen productivity
1157 estimates for common taxa of the northern Siberian Arctic, *Rev. Palaeobot. Palynol.*, 221, 71–82,
1158 <https://doi.org/10.1016/j.revpalbo.2015.06.008>, 2015.

1159 Nikulina, A., MacDonald, K., Zapolska, A., Serge, M. A., Roche, D. M., Mazier, F., Davoli, M.,
1160 Svenning, J.-C., van Wees, D., Pearce, E. A., Fyfe, R., Roebroeks, W., and Scherjon, F.: Hunter-
1161 gatherer impact on European interglacial vegetation: A modelling approach, *Quat. Sci. Rev.*, 324,
1162 108439, <https://doi.org/10.1016/j.quascirev.2023.108439>, 2024.

1163 Ninyerola, M., i Fernández, X. P., and Roure, J. M.: Atlas climático digital de la Península Ibérica:
1164 metodología y aplicaciones en bioclimatología y geobotánica, 2005.

1165 Paciorek, C. J. and McLachlan, J. S.: Mapping Ancient Forests: Bayesian Inference for Spatio-
1166 Temporal Trends in Forest Composition Using the Fossil Pollen Proxy Record, *J. Am. Stat. Assoc.*, 104, 608–622, <https://doi.org/10.1198/jasa.2009.0026>, 2009.

1168 Parsons, R. W. and Prentice, I. C.: Statistical approaches to R-values and the pollen— vegetation
1169 relationship, *Rev. Palaeobot. Palynol.*, 32, 127–152, [https://doi.org/10.1016/0034-6667\(81\)90001-4](https://doi.org/10.1016/0034-6667(81)90001-4), 1981.

1171 Pearce, E. A., Mazier, F., Normand, S., Fyfe, R., Andrieu, V., Bakels, C., Balwierz, Z., Bińka,
1172 K., Boreham, S., Borisova, O. K., Brostrom, A., de Beaulieu, J.-L., Gao, C., González-Sampériz,
1173 P., Granoszewski, W., Hrynowiecka, A., Kołaczek, P., Kuneś, P., Magri, D., Malkiewicz, M.,
1174 Mighall, T., Milner, A. M., Möller, P., Nita, M., Noryśkiewicz, B., Pidek, I. A., Reille, M.,
1175 Robertsson, A.-M., Salonen, J. S., Schläfli, P., Schokker, J., Scussolini, P., Šeirienė, V., Strahl,
1176 J., Urban, B., Winter, H., and Svenning, J.-C.: Substantial light woodland and open vegetation
1177 characterized the temperate forest biome before *Homo sapiens*, *Sci. Adv.*, 9, eadi9135,
1178 <https://doi.org/10.1126/sciadv.adi9135>, 2023.

1179 Pearce, E. A., Mazier, F., Davison, C. W., Baines, O., Czyżewski, S., Fyfe, R., Bińka, K.,
1180 Boreham, S., De Beaulieu, J.-L., Gao, C., Granoszewski, W., Hrynowiecka, A., Malkiewicz, M.,
1181 Mighall, T., Noryśkiewicz, B., Pidek, I. A., Strahl, J., Winter, H., and Svenning, J.-C.: Beyond
1182 the closed-forest paradigm: Cross-scale vegetation structure in temperate Europe before the late-
1183 Quaternary megafauna extinctions, *Earth Hist. Biodivers.*, 3, 100022,
1184 <https://doi.org/10.1016/j.hisbio.2025.100022>, 2025a.

1185 Pearce, E. A., Davison, C. W., Mazier, F., Normand, S., Fyfe, R., Serge, M., Scussolini, P., and
1186 Svenning, J.: Drivers of Vegetation Structure Differ Between Proposed Natural Reference

1187 Conditions for Temperate Europe, *Glob. Ecol. Biogeogr.*, 34, <https://doi.org/10.1111/geb.70020>,
1188 2025b.

1189 Pérez-Obiol, R., Jalut, G., Julià, R., Pèlachs, A., Iriarte, M. J., Otto, T., and Hernández-Beloqui,
1190 B.: Mid-Holocene vegetation and climatic history of the Iberian Peninsula, *The Holocene*, 21,
1191 75–93, <https://doi.org/10.1177/0959683610384161>, 2011.

1192 Pirzamanbein, B., Lindström, J., Poska, A., Sugita, S., Trondman, A.-K., Fyfe, R., Mazier, F.,
1193 Nielsen, A. B., Kaplan, J. O., Bjune, A. E., Birks, H. J. B., Giesecke, T., Kangur, M., Latałowa,
1194 M., Marquer, L., Smith, B., and Gaillard, M.-J.: Creating spatially continuous maps of past land
1195 cover from point estimates: A new statistical approach applied to pollen data, *Ecol. Complex.*,
1196 20, 127–141, <https://doi.org/10.1016/j.ecocom.2014.09.005>, 2014.

1197 Pirzamanbein, B., Poska, A., and Lindström, J.: Bayesian Reconstruction of Past Land Cover
1198 From Pollen Data: Model Robustness and Sensitivity to Auxiliary Variables, *Earth Space Sci.*, 7,
1199 e2018EA00057, <https://doi.org/10.1029/2018EA000547>, 2020.

1200 Poska, A., Meltssov, V., Sugita, S., and Vassiljev, J.: Relative pollen productivity estimates of
1201 major anemophilous taxa and relevant source area of pollen in a cultural landscape of the hemi-
1202 boreal forest zone (Estonia), *Rev. Palaeobot. Palynol.*, 167, 30–39,
1203 <https://doi.org/10.1016/j.revpalbo.2011.07.001>, 2011.

1204 Prentice, I. C. and Parsons, R. W.: Maximum Likelihood Linear Calibration of Pollen Spectra in
1205 Terms of Forest Composition, *Biometrics*, 39, 1051–1057, <https://doi.org/10.2307/2531338>,
1206 1983.

1207 Prentice, I. C. and Webb, T.: Pollen percentages, tree abundances and the Fagerlind effect, *J.
1208 Quat. Sci.*, 1, 35–43, <https://doi.org/10.1002/jqs.3390010105>, 2009.

1209 R Core Team: _R: A Language and Environment for Statistical Computing. R Foundation for
1210 Statistical Computing, 2025.

1211 Reille, M.: Pollen et spores d'europe et d'afrique du nord, Laboratoire de Botanique historique et
1212 Palynologie, Marseille, 1992.

1213 Reille, M.: Pollen et spores d'europe et d'afrique du nord, supplement 1, Laboratoire de Botanique
1214 historique et Palynologie, Marseille, 1995.

1215 Roberts, N., Fyfe, R. M., Woodbridge, J., Gaillard, M.-J., Davis, B. A. S., Kaplan, J. O., Marquer,
1216 L., Mazier, F., Nielsen, A. B., Sugita, S., Trondman, A.-K., and Leydet, M.: Europe's lost forests:
1217 a pollen-based synthesis for the last 11,000 years, *Sci. Rep.*, 8, 716,
1218 <https://doi.org/10.1038/s41598-017-18646-7>, 2018.

1219 Rubiales, J. M., García-Amorena, I., Hernández, L., Génova, M., Martínez, F., Manzaneque, F.
1220 G., and Morla, C.: Late Quaternary dynamics of pinewoods in the Iberian Mountains, *Rev.
1221 Palaeobot. Palynol.*, 162, 476–491, <https://doi.org/10.1016/j.revpalbo.2009.11.008>, 2010.

1222 Serge, M., Mazier, F., Fyfe, R., Gaillard, M.-J., Klein, T., Lagnoux, A., Galop, D., Githumbi, E.,
1223 Mindrescu, M., Nielsen, A., Trondman, A.-K., Poska, A., Sugita, S., Woodbridge, J., Abel-
1224 Schaad, D., Åkesson, C., Alenius, T., Ammann, B., Andersen, S., Anderson, R., Andrić, M.,
1225 Balakauskas, L., Barnekow, L., Batalova, V., Bergman, J., Birks, H., Björkman, L., Bjune, A.,
1226 Borisova, O., Broothaerts, N., Carrion, J., Caseldine, C., Christiansen, J., Cui, Q., Currás, A.,
1227 Czerwiński, S., David, R., Davies, A., De Jong, R., Di Rita, F., Dietre, B., Dörfler, W., Doyen,
1228 Edwards, K., Ejarque, A., Endtmann, E., Etienne, D., Faure, E., Feeser, I., Feurdean, A.,
1229 Fischer, E., Fletcher, W., Franco-Múgica, F., Fredh, E., Froyd, C., Garcés-Pastor, S., García-

1230 Moreiras, I., Gauthier, E., Gil-Romera, G., González-Sampériz, P., Grant, M., Grindean, R., Haas,
1231 J., Hannon, G., Heather, A.-J., Heikkilä, M., Hjelle, K., Jahns, S., Jasiunas, N., Jiménez-Moreno,
1232 G., Jouffroy-Bapicot, I., Kabailiené, M., Kamerling, I., Kangur, M., Karpińska-Kołaczek, M.,
1233 Kasianova, A., Kołaczek, P., Lagerås, P., Latalowa, M., Lechterbeck, J., Leroyer, C., Leydet, M.,
1234 Lindbladh, M., Lisitsyna, O., López-Sáez, J.-A., Lowe, J., Luelmo-Lautenschlaeger, R.,
1235 Lukáňa, E., Maciáuskaité, L., Magri, D., Marguerie, D., Marquer, L., Martinez-Cortizas, A.,
1236 Mehl, I., Mesa-Fernández, J., Mighall, T., Miola, A., Miras, Y., Morales-Molino, C., et al.:
1237 Testing the Effect of Relative Pollen Productivity on the REVEALS Model: A Validated
1238 Reconstruction of Europe-Wide Holocene Vegetation, *Land*, 12, 986,
1239 <https://doi.org/10.3390/land12050986>, 2023.

1240 Soepboer, W., Sugita, S., Lotter, A. F., van Leeuwen, J. F. N., and van der Knaap, W. O.: Pollen
1241 productivity estimates for quantitative reconstruction of vegetation cover on the Swiss Plateau,
1242 *The Holocene*, 17, 65–77, <https://doi.org/10.1177/0959683607073279>, 2007.

1243 Sugita, S.: Pollen representation of vegetation in Quaternary sediments: theory and method in
1244 patchy vegetation, *J. Ecol.*, 82, 881–897, <https://doi.org/10.2307/2261452>, 1994.

1245 Sugita, S.: Theory of Quantitative Reconstruction of Vegetation I: Pollen from Large Sites
1246 REVEALS Regional Vegetation Composition, *The Holocene*, 17, 229–241,
1247 <https://doi.org/10.1177/0959683607075837>, 2007a.

1248 Sugita, S.: Theory of Quantitative Reconstruction of Vegetation II: All You Need Is LOVE, *The
1249 Holocene*, 17, 243–257, <https://doi.org/10.1177/0959683607075838>, 2007b.

1250 Sugita, S., Parshall, T., Calcote, R., and Walker, K.: Testing the Landscape Reconstruction
1251 Algorithm for spatially explicit reconstruction of vegetation in northern Michigan and Wisconsin,
1252 *Quat. Res.*, 74, 289–300, <https://doi.org/10.1016/j.yqres.2010.07.008>, 2010.

1253 Svenning, J.-C.: A review of natural vegetation openness in north-western Europe, *Biol. Conserv.*,
1254 104, 133–148, [https://doi.org/10.1016/S0006-3207\(01\)00162-8](https://doi.org/10.1016/S0006-3207(01)00162-8), 2002.

1255 Tabares, X., Ratzmann, G., Kruse, S., Theuerkauf, M., Mapani, B., and Herzschuh, U.: Relative
1256 pollen productivity estimates of savanna taxa from southern Africa and their application to
1257 reconstruct shrub encroachment during the last century, *The Holocene*, 31, 1100–1111,
1258 <https://doi.org/10.1177/09596836211003193>, 2021.

1259 Theuerkauf, M.: Pollen productivity estimates, in: *Encyclopedia of Quaternary Science*, Elsevier,
1260 387–401, <https://doi.org/10.1016/B978-0-323-99931-1.00236-1>, 2025.

1261 Theuerkauf, M. and Couwenberg, J.: The extended downscaling approach: A new R-tool for
1262 pollen-based reconstruction of vegetation patterns, *The Holocene*, 27, 1252–1258,
1263 <https://doi.org/10.1177/0959683616683256>, 2017.

1264 Theuerkauf, M. and Couwenberg, J.: ROPES Reveals Past Land Cover and PPEs From Single
1265 Pollen Records, *Front. Earth Sci.*, 6, 14, <https://doi.org/10.3389/feart.2018.00014>, 2018.

1266 Theuerkauf, M. and Couwenberg, J.: Pollen productivity estimates strongly depend on assumed
1267 pollen dispersal II: Extending the ERV model, *The Holocene*, 32, 1233–1250,
1268 <https://doi.org/10.1177/09596836211041729>, 2022.

1269 Theuerkauf, M., Kuparinen, A., and Joosten, H.: Pollen productivity estimates strongly depend
1270 on assumed pollen dispersal, *The Holocene*, 23, 14–24,
1271 <https://doi.org/10.1177/0959683612450194>, 2013.

1272 Theuerkauf, M., Bos, J. A. A., Jahns, S., Janke, W., Kuparinen, A., Stebich, M., and Joosten, H.:
1273 *Corylus* expansion and persistent openness in the early Holocene vegetation of northern central
1274 Europe, *Quat. Sci. Rev.*, 90, 183–198, <https://doi.org/10.1016/j.quascirev.2014.03.002>, 2014.

1275 Theuerkauf, M., Couwenberg, J., Kuparinen, A., and Liebscher, V.: A matter of dispersal:
1276 REVEALSSinR introduces state-of-the-art dispersal models to quantitative vegetation
1277 reconstruction, *Veg. Hist. Archaeobotany*, 25, 541–553, <https://doi.org/10.1007/s00334-016-0572-0>, 2016.

1279 Trachsel, M., Dawson, A., Paciorek, C. J., Williams, J. W., McLachlan, J. S., Cogbill, C. V.,
1280 Foster, D. R., Goring, S. J., Jackson, S. T., Oswald, W. W., and Shuman, B. N.: Comparison of
1281 settlement-era vegetation reconstructions for STEPPS and REVEALS pollen–vegetation models
1282 in the northeastern United States, *Quat. Res.*, 95, 23–42, <https://doi.org/10.1017/qua.2019.81>,
1283 2020.

1284 Trondman, A.-K., Gaillard, M.-J., Mazier, F., Sugita, S., Fyfe, R., Nielsen, A. B., Twiddle, C.,
1285 Barratt, P., Birks, H. J. B., Bjune, A. E., Björkman, L., Broström, A., Caseldine, C., David, R.,
1286 Dodson, J., Dörfler, W., Fischer, E., van Geel, B., Giesecke, T., Hultberg, T., Kalnina, L., Kangur,
1287 M., van der Knaap, P., Koff, T., Kuneš, P., Lagerås, P., Latałowa, M., Lechterbeck, J., Leroyer,
1288 C., Leydet, M., Lindbladh, M., Marquer, L., Mitchell, F. J. G., Odgaard, B. V., Peglar, S. M.,
1289 Persson, T., Poska, A., Rösch, M., Seppä, H., Veski, S., and Wick, L.: Pollen-based quantitative
1290 reconstructions of Holocene regional vegetation cover (plant functional types and land-cover
1291 types) in Europe suitable for climate modelling, *Glob. Change Biol.*, n/a-n/a,
1292 <https://doi.org/10.1111/gcb.12737>, 2014.

1293 Trondman, A.-K., Gaillard, M.-J., Mazier, F., Sugita, S., Fyfe, R., Nielsen, A. B., Twiddle, C.,
1294 Barratt, P., Birks, H. J. B., Bjune, A. E., Björkman, L., Broström, A., Caseldine, C., David, R.,
1295 Dodson, J., Dörfler, W., Fischer, E., van Geel, B., Giesecke, T., Hultberg, T., Kalnina, L., Kangur,
1296 M., van der Knaap, P., Koff, T., Kuneš, P., Lagerås, P., Latałowa, M., Lechterbeck, J., Leroyer,
1297 C., Leydet, M., Lindbladh, M., Marquer, L., Mitchell, F. J. G., Odgaard, B. V., Peglar, S. M.,
1298 Persson, T., Poska, A., Rösch, M., Seppä, H., Veski, S., and Wick, L.: Pollen-based quantitative
1299 reconstructions of Holocene regional vegetation cover (plant-functional types and land-cover
1300 types) in Europe suitable for climate modelling, *Glob. Change Biol.*, 21, 676–697,
1301 <https://doi.org/10.1111/gcb.12737>, 2015.

1302 Veeken, A., Santos, M. J., McGowan, S., Davies, A. L., and Schrodt, F.: Pollen-based
1303 reconstruction reveals the impact of the onset of agriculture on plant functional trait composition,
1304 *Ecol. Lett.*, 25, 1937–1951, <https://doi.org/10.1111/ele.14063>, 2022.

1305 Vera, F. W. M.: *Grazing ecology and forest history*, CABI Pub, Wallingford, Oxon ; New York,
1306 NY, 506 pp., 2000.

1307 Von Post, L.: Skogsträdpollen i sydsvenska torvmosselagerföljder, *Forhandlinger ved de*, 16,
1308 433–465, 1918.

1309 Wan, Q., Zhang, X., Huang, K., Zheng, H., Zhang, Y., Yang, X., and Zheng, Z.: Validation of
1310 relative pollen productivities for major tropical plant taxa: An empirical test using the REVEALS
1311 model in Hainan, China, *Quat. Int.*, 641, 106–114, <https://doi.org/10.1016/j.quaint.2022.04.006>,
1312 2022.

1313 Wieczorek, M. and Herzschuh, U.: Compilation of relative pollen productivity (RPP) estimates
1314 and taxonomically harmonised RPP datasets for single continents and Northern Hemisphere
1315 extratropics, *Earth Syst. Sci. Data*, 12, 3515–3528, <https://doi.org/10.5194/essd-12-3515-2020>,
1316 2020.

1317 Woodbridge, J., Roberts, C. N., Palmisano, A., Bevan, A., Shennan, S., Fyfe, R., Eastwood, W.
1318 J., Izdebski, A., Çakırlar, C., Woldring, H., Broothaerts, N., Kaniewski, D., Finné, M., and
1319 Labuhn, I.: Pollen-inferred regional vegetation patterns and demographic change in Southern
1320 Anatolia through the Holocene, *The Holocene*, 29, 728–741,
1321 <https://doi.org/10.1177/0959683619826635>, 2019.

1322 Xiang, Y., Gubian, S., Suomela, B., and Hoeng, J.: Generalized Simulated Annealing for Global
1323 Optimization: The GenSA Package, *R J.*, 5, 13, <https://doi.org/10.32614/RJ-2013-002>, 2013.

1324 Xu, Q., Cao, X., Tian, F., Zhang, S., Li, Y., Li, M., Li, J., Liu, Y., and Liang, J.: Relative pollen
1325 productivities of typical steppe species in northern China and their potential in past vegetation
1326 reconstruction, *Sci. China Earth Sci.*, 57, 1254–1266, <https://doi.org/10.1007/s11430-013-4738-7>, 2014.

1328 Zanon, M., Davis, B. A. S., Marquer, L., Brewer, S., and Kaplan, J. O.: European Forest Cover
1329 During the Past 12,000 Years: A Palynological Reconstruction Based on Modern Analogs and
1330 Remote Sensing, *Front. Plant Sci.*, 9, 253, <https://doi.org/10.3389/fpls.2018.00253>, 2018.

1331

1332

1333

1334